AN EMPIRICAL ASSESSMENT OF THE SHEAR STRENGTH OF ROCK DISCONTINUITIES AT NCHANGA OPEN PIT MINE

By

Fexon Mondoka

A Dissertation submitted to the University of Zambia in partial fulfilment of the requirements of the degree of MASTER of MINERAL SCIENCES

THE UNIVERSITY OF ZAMBIA

LUSAKA

1988

DECLARATION

I, **Fexon Mondoka**, hereby declare that this dissertation is my own work and that it has not been submitted, in part or in full, for a degree at the University of Zambia or any other University.

Signature

APPROVAL

This dissertation of **Fexon Mondoka** is approved as fulfilling part of the requirements for the award of the degree of **Master of Mineral Sciences in Rock Mechanics** by the University of Zambia.

Signature of Examiner	Date of Approval
Signature	Date
Signature	Date

Abstract

An empirical assessment of the peak shear strength of rock discontinuities occuring in the hangingwall rock formations at Nchanga Open Pit is presented in this dissertation.

A brief history and geology of the open pit including its structural and geometrical setting are outlined. Some recent slope failures have been included to show the trend in the mechanism of failure.

All discontinuities occuring in the rock masses have been summarized under two types. Type 1 covers all natural planes of weakness such as joints, minor faults, bedding and cleavage planes. Type 2 includes all artificial fractures such as through-going tension cracks and fractures resulting from blast damage. The description of the rock types follows local nomenclature.

The shear strength behaviour of the two types of discontinuities has been defined following the empirical shear strength criterion. The criterion is expressed as an equation based on three index parameters controlling the shear behaviour of a discontinuity or joint, namely:

(i) the joint roughness coefficient (JRC),
(ii) the joint wall compressive strength (JCS), and
(iii) the residual angle of internal friction (ϕr).

These index parameters were determined following experimental procedures proposed by Barton and Choubey (1977).

The results of the field and laboratory measurements conducted for the determination of these index parameters are presented both in tabular and graphical forms. Mean values of these index parameters have been applied into the 'empirical equation' defining the peak shear strength of a discontinuity in terms of a total friction angle (arctan $\tau/\sigma n$). This equation has further been interpreted into a log-tan chart. The chart has a logarithmic scale on the ordinate and a tangent scale on the abscissa. Plots of the governing stress ratios, $JCS/\sigma n$ and $\tau/\sigma n$ which are the joint compressive strength and shear strength to effective normal stress ratios, are presented on the charts.

Five rock types were represented in the investigation; the Shale with Grit (SWG), Chingola Dolomite (C/DOL), Dolomitic Schist (DOLSCHIST), Upper Banded Shale (UBS), and the Feldspathic Quartzite (TFQ). For each of the five rock types, a log-tan chart has been plotted to define the peak shear strength criterion for its Type 1 and Type 2 discontinuities. The range of friction angles obtainable from a graphical interpretation of the charts is shown to compare well with values already in design use on the Mine. The added advantage resulting from the findings of this study is that, reliable predictions of the shear strength information pertaining to the five rock formations represented in the investigation can now be made.

Acknowledgements

The results of this work, and the theory and experiment relevant to the study, are described in a great number of papers scattered over many scientific and engineering journals and texts, and the proceedings of several conferences and symposia on the subject of rock mechanics. Some of these papers are listed in the Bibliography, and I would like to express my gratitude to the authors of the same.

However, specific appreciations have been reserved for the following:

(i) My employers, **Zambia Consolidated Copper Mines Ltd.**, for their sponsorship and having made available laboratory facilities for use.

(ii) **Dr M.W. Chanda** for his supervisory work and for taking a keen interest in going through the project scripts, and for his valuable comments.

(iii) My course mates, **Yost Kalasa** and **Robert Kamanga**, for the fruitful interchange of ideas.

(iv) My wife, **Rabecca** and our two children **Chadli** and **Peverly**, for their perseverance.

(v) The Soils Analyst, **Wellington Sichilima**, for his assistance during field and laboratory work.

(vi) Lastly but not least, to **Joseph Kabotolo** for proof-reading the report.

Table of Contents

Chapter 1

Introduction

Most of the engineering problems encountered in both underground and surface excavations are largely influenced by the shear behaviour of the discontinuity network inherent in the surrounding wall rocks. When assessing the shear strength properties of rock masses one is actually dealing with the shear behaviour of the rock discontinuities.

For the purpose of this study, the term 'discontinuity' is used to define any structural plane of weakness in rock upon which movement can take place. These weakness planes may have occured either by natural or/and artificial processes causing a break in the body of rock. They usually exhibit zero or low tensile strengths under tests. Bedding planes, cleavage, joints, minor faults and tension cracks through intact rock are of the sort.

Associated with any discontinuity is the roughness of its walls characterized by waveness and unevenness, simply termed the 'surface roughness'. This is described as a potentially important component of the shear strength of a discontinuity (Brown 1981). Because of the strong influence of the surface roughness, rock discontinuities exhibit a wide spectrum of shear strength under low levels of the effective normal stress. Conversely, under high levels of normal stress the shear strength spectrum is narrowed.

The criterion of failure in rock slopes is that the rock mass behind the slope should become unstable. This happens when it experiences a fall in the peak shear strength to a residual value as a result of additional displacements taking place locally along favourably oriented discontinuities. How large the displacements should be in order to mobilize sufficient residual strength before overall failure is, to some extent, a function of the surface roughness of the overstressed discontinuities and the magnitude of the effective normal stresses acting in relation to the compressive strength of the discontinuity walls.

From the results of many experimental investigations in this field, it has been recommended to include the influence of 'surface roughness' in defining the shear strength of discontinuities (Brown 1981). Empirical laws of friction and fracture have been developed from laboratory-scale tests on rock and rock joints to provide an adequate definition of the shear strength of discontinuities. Notable among these empirical laws is the 'Empirical Shear Strength Criterion' formulated by Barton (1973), later joined by Choubey (1977). In rock mechanics, the aim is to employ quicker and cheaper quantitative methods of obtaining rock strength parameters for use in design. Barton's empirical shear strength criterion is one of such methods. It estimates the peak

shear strength, which can be measured, in a rock discontinuity with its included surface roughness, in a given working range of the effective normal stress.

This work, attempts to make a quantitative assessment of peak shear strength properties of rock discontinuities governing the shear behaviour of the Nchanga Open Pit (NOP) hangingwall, following the empirical shear strength approach (Barton and Choubey 1977). The discontinuities have been described under two types; Type 1 - those which are naturally occuring, and Type 2 - those which are artificially induced. Testwork involved simple field and laboratory strength index tests using simple equipment such as the Point Load Machine (Plate No.1); Shear-Box (Plate No.2) and the Schmidt Hammer.

In order to narrow variations in the strength values obtained from laboratory and field measurements, sampling was concentrated between section lines 6E and 9E of the Nchanga Open Pit hanging wall. Plate Nos.3 and 4 show part of the sampled face.

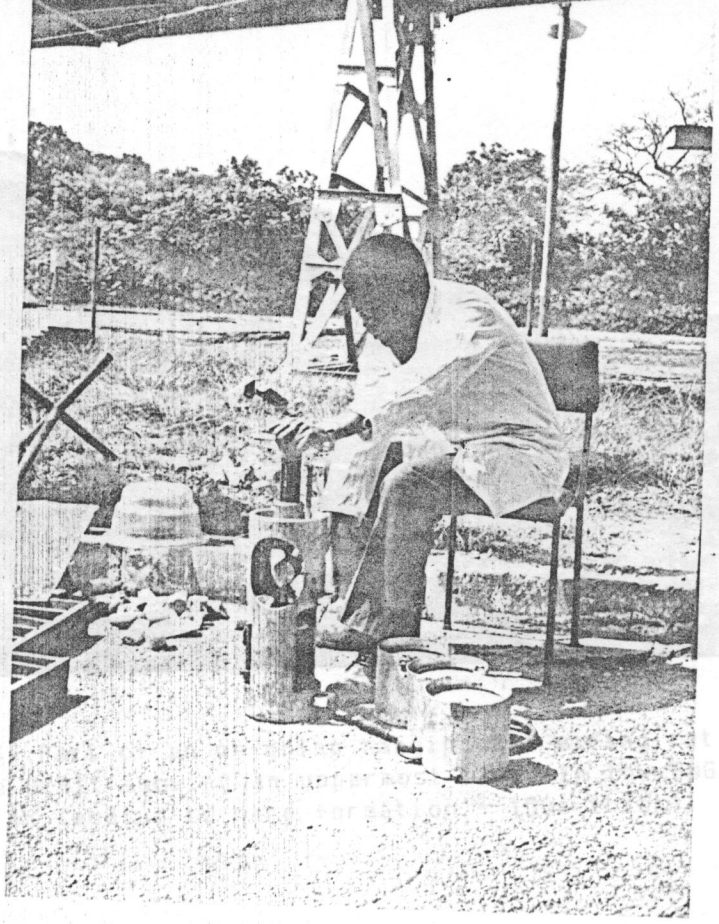

Plate 1: Testing core samples of rock for strngth index with Point Load Machine.

Plate 2: Testing prepared core samples of rock for shear strength parameters "C" & "ϕ" with a Shear-Box unit.

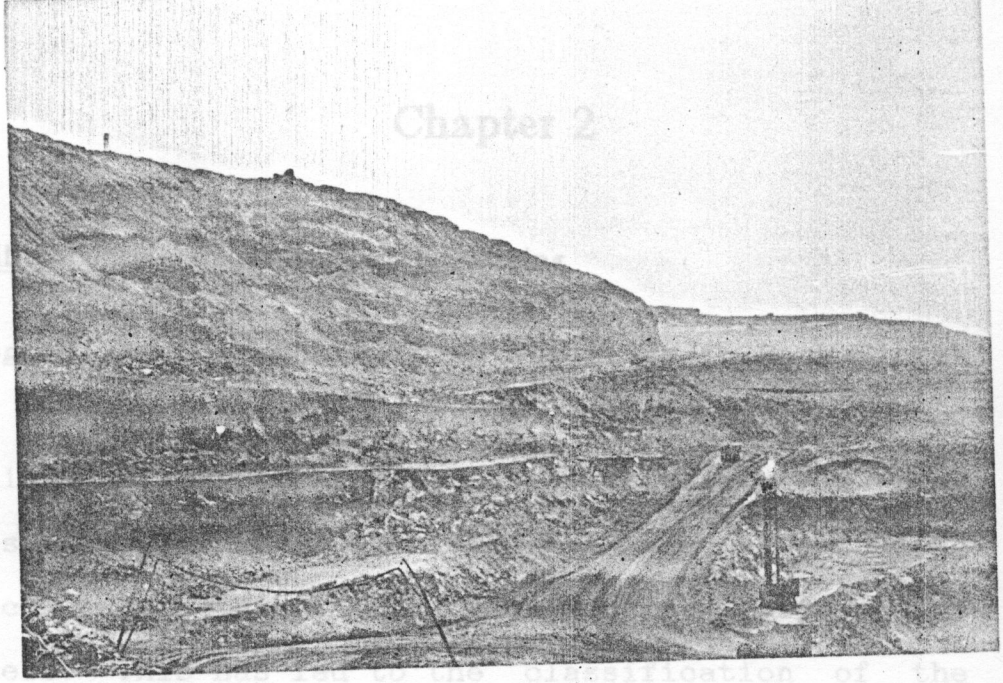

Plate 3: Part of an on-going hangingwall mining cut at Nchanga O/Pit showing an uppermost slope in the SWG formation (medium to hard formation - 150m thick).

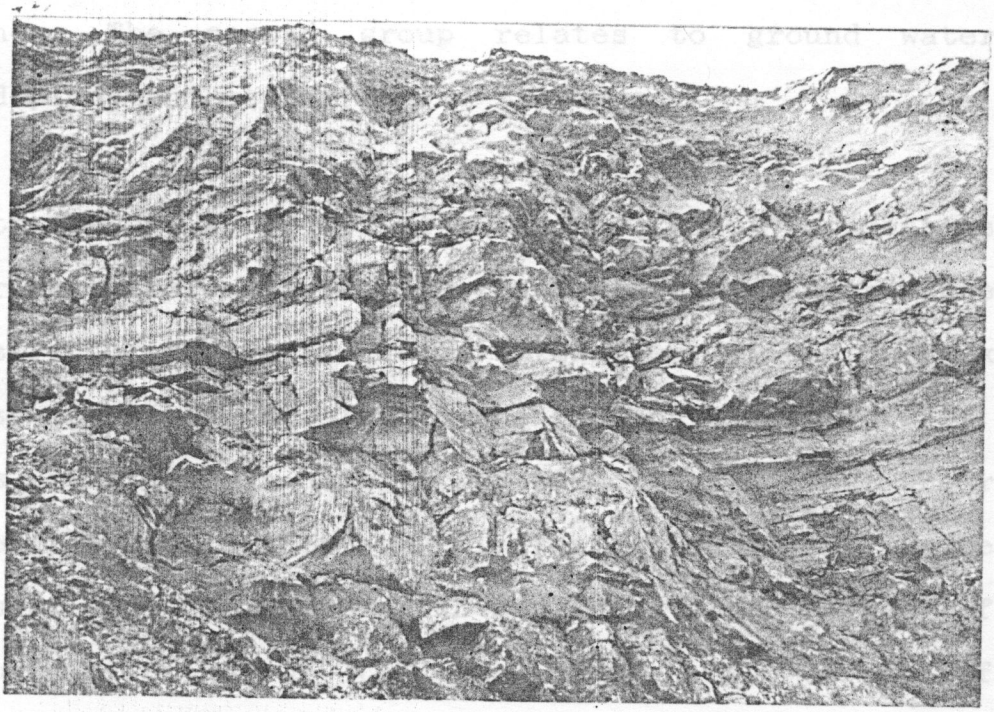

Plate 4: A full bench face showing bedding, jointing and folding in the Dolomitic Schist formation (hard formation: 15 - 120m thick).

Chapter 2

General Stability Considerations in Open Pit Mining

2.1 Geological Factors Controlling Stability in Rock Slopes

The distinguishing feature of slope stability in rock slopes is that most of the failures take place along surfaces coinciding with pre-existing planes of weakness. This has led to the classification of the geological factors influencing stability in rock slopes into two main groups (Patton and Deere 1970). The first group includes the omnipresent structural defects such as: through-going joints, faults, cleavage and bedding planes. The second group relates to ground water conditions and weathering.

In the second group; critical ground water conditions in rock slopes, are often a consequence of the presence of structural defects. Water pressures within a rock mass act perpendicular to the discontinuity planes. This results in a significant reduction of the shear strength. Many different geological conditions can be present in local areas which may result in a variety of slope failures. On the other hand, the effect of weathering on a rock mass is to degrade its strength and change its deformability and permeability characteristics. As a result, the influence of the irregularities characterising joint surfaces is diminished as the strength of the material forming the

surfaces is reduced. The probability of the joint irregularities shearing-off rather than being over-ridden at failure is thus increased. Weathering also tends to form zones of materials with different permeabilities which may give rise to varying pore water pressures within the same horizon.

2.2 The Criterion of Failure in Rock Slopes

A rock mass becomes unstable when it experiences a fall in the peak shear strength to a residual value. This is usually caused by additional displacements taking place locally along discontinuities, influenced by the removal of an adjacent ground mass through excavation or other natural processes taking place in the earth's crust. The amount of displacement required to mobilise the residual strength before overall failure depends, to some extent, on the roughness and degree of undulation of the over-stressed discontinuities and on the level of the effective normal stress relative to the discontinuity wall strength. In agreement with Patton and Deere (1970), typical rock slope failures can be summarised under three categories as folows:

(i) Category A - Localised slope failures
(ii) Category B - Large-scale wedge failures
(iii) Category C - Circular failures.

2.2.1 Local Slope Failures

Local failures of small rock masses along one or more discontinuity planes are common in any large excavation. They are impossible to eliminate. The worst problem presented by these local failures is that of hazard to men and equipment. They usually occur in a plane failure mode involving one or two benches off a continuous rock slope.

2.2.2 Large-scale Wedge Failures

The presence of two or more planar discontinuities striking obliquely across the slope face, may lead to a large-scale wedge failure. This happens when their line of intersection daylights in the slope face at an inclination greater than the angle of friction of the rock material. This structural condition is potentially more hazardous than the localised one since a voluminous amount of ground may become involved in the slide.

2.2.3 Circular Failures

These failures occur where pit slopes encounter wide fault zones containing sheared and decomposed rock. They also take place in weak and heavily jointed rock masses. The slope may not fail until the excavation has considerably proceeded down to a certain elevation at which the failure plane would toe out. These failures, generally, mobilise huge amounts of ground material and more often severely affect mining operations.

2.3 Influence of Blasting on the Stability of Rock Slopes

One of the major problems that arises from the excavation of rock slopes is that the very material intended to remain stable is, in most cases, left seriously damaged by the seismic shocks generated by blasting operations. Two types of unwanted damage which result from blasting operations are:

(i) Damage to existing slopes and structures and
(ii) Fracturing of rock beyond excavation limits.

These problems are especially acute nowadays when blasting operations have assumed greater dimensions. Large diameter holes and increased bench heights requiring increased explosive loads per hole are widely employed in the design of large open pit blasts. Hence, the rapture radius for a single blast hole has increased along with the vibration level produced per hole.

Unfortunately, many rock mechanics engineers often ignore the seismic influence when analysing slopes with respect to stability. However, it is a well known fact that the entire stability force system dramatically changes when acted upon by a blast-acceleration pulse. This was shown by Calder and Bauer (1970) to have a net effect in a large reduction of the factor of safety.

Nevertheless, blasting control techniques have since been devised to minimise the two types of unwanted damage enumerated above. It has been established that the vibration effects are strongly influenced by the weight of the charge per hole, the number of holes per delay, the distance from the shot point, the mode of initiation and the point of interest in relation to the blast (Edwards and Northwood 1960; Duvall and Fogelson 1962). In order to minimise vibration effects, various blast-hole patterns are designed according to ground conditions with emphasis on delay and sequence blasting to achieve the objective. {At Nchanga Open Pit, common blast-hole sizes and patterns, in type of ground, are: 229mm hole diameter = 7 metre-burden by 8.75 metre-spacing in soft to medium hard ground; and 6m by 7.5m in hard ground. 311mm hole dia. = 8m by 10m in soft to medium hard ground; 7m by 8.75m in hard ground. Anfex is the main explosive} The type of charge (e.g crater or cylinder) and its size have been linked with causing fracturing of ground beyond excavation limits. In order to arrest this effect, control blasting methods such as; cushion blasting, pre-split blasting and buffer blasting have been devised.

Chapter 3

Review of the Rockmass Shear Strength Theory and Strength Tests

3.1 Introduction

The shear strength of a rock mass is generally measured by the shear strength of a through-going discontinuity. The geometrical relationship between the breaks in the rock mass and the slope and orientation of the excavated face will determine whether parts of the rock mass are free to slide or fall. This is a measure of the shear strength of the rock mass in question.

Determination of the shear strength mobilised at failure in various rock types is a critical part of slope design. A potential failure surface, which may be a single discontinuity plane or a complex path following several discontinuities and involving some fracture of the intact material, might be considered. The choice of appropriate shear strength values for use does not only depend upon the available test data but also upon a careful interpretation of these data in relation to the behaviour of the rock mass forming the full-scale slope (Hoek and Bray 1981).

It is possible to use the test data obtained from direct shear tests in designing a slope in which failure is likely to occur along a single discontinuity plane similar to the one tested. However, the same

values could not be used directly in designing a slope in which a complex failure process is anticipated. Such a failure may involve several discontinuities and some fracture through intact rock. In this case some modifications would have to be made to the shear strength data in order to account for the difference in the shear strengths of the discontinuities involved.

It is customary to fit Coulomb's linear relationship:

$$\tau = c + \sigma_n . \tan\phi \quad \ldots\ldots\ldots\ldots\ldots\ldots\ldots\ldots (1)$$

to the results of shear strength investigations on rock discontinuities. [τ = peak shear strength (MPa); c = cohesion intercept (MPa); σ_n = normal stress; ϕ = angle of internal friction] Characterising the surface of a discontinuity is its roughness. The wall roughness is a potentially important component of the shear strength of any rock discontinuity. If, for example, equation (1) is applied to the results of shear tests on rough-undulating discontinuities, under both high and low levels of the normal stress, differing results would be obtained.

This fact was recognized by Jaeger (1959), Krsmanovic and Langof (1964) and Barton (1971a), and by increasing

numbers of investigators during the past 20 years. However, the habit remains that of describing the shear strength in terms of Coulomb's constants 'c' and 'ϕ'. Both are stress dependent variables. They are also scale dependent (Barton, Bandis and Lumsden 1981).

3.2 The Peak Shear Strength Criterion

The peak shear strength criterion is a shear strength theory based on the empirical laws of friction and fracture applicable to rock and rock discontinuities. Barton N.R. has been instrumental in the formulation of this theory. The theory is widely applied in many shear strength investigations for most rock engineering problems.

Rock discontinuities exhibit a wide spectrum of shear strength under low effective normal stress levels. This is due to the strong influence of the surface roughness and the variable rock strength. Conversely, under high effective normal stress levels the shear strength spectrum is narrow despite variations in the compressive strength of rocks at failure. Thus, another factor affecting the shear strength is the magnitude of the effective normal stress (σ_n) acting across the discontinuity.

Before introducing a more satisfactory method of describing the shear strength of rock discontinuities an empirical approach was considered (Barton 1973). This was dictated by the fact that stability calculations both in soil and rock mechanics are carried out in terms of 'conventional' stresses. Mathematically, that is to say, a given stress level is equal to effective load divided by gross area, with no consideration for the microscopic or visible contact area. The contact area involved when shearing rock discontinuities is extremely small and may be anything from one tenth to one thousandth or less of the gross area as shown, for example, by Jaeger (1971) and Barton (1971a). Thus, in a typical rock mechanics problem the actual shear and normal stresses acting across the discontinuity asperities, visibly in contact, can be as much as a thousand times higher than the 'conventional' ones.

3.2.1 The Empirical Equation of Shear Strength

To describe the shear strength of rock joints satisfactorily, Barton (1973) formulated an empirical relationship based on three index parameters, namely:

(i) the joint roughness coefficient (JRC)

(ii) the joint wall compressive strength (JCS)

(iii) the basic angle of internal friction (ϕb).

This relationship is expressed in the following equation:

$$\tau = \sigma n . \tan[JRC . Log(JCS/\sigma n) + \phi b] \quad .....(2)$$

where τ = peak shear strength

σn = effective normal stress.

In later investigations (Barton and Choubey 1977), it was preferred to substitute the residual angle of internal friction ϕr for ϕb since rock joint walls are generally weathered to some extent. ϕr was thus defined as a minimum intrinsic shear strength property of a rock joint (ϕr is less than or equal to ϕb). Equation (2) becomes:

$$\tau = \sigma n . \tan[JRC . Log(JCS/\sigma n) + \phi r] \quad .....(3)$$

This empirical relationship can be used both to fit or extrapolate experimental data and to predict it. The three index parameters; JRC, JCS, and ϕr can be obtained from simple laboratory tests.

3.2.2 Determination of the Strength Index Parameters

I. Joint Roughness Coefficient (JRC)

The waveness and unevenness of the joint or discontinuity surfaces constitute their roughness. JRC is an empirical quantity and it is simply a number between 0 and 20 represented on a comprehensive set of standard roughness profiles (Fig.1). The larger the number the rougher the surface. The International Society of Rock Mechanics (Brown 1981) recommends three methods for sampling roughness, and these are:

(i) Linear profiling along direction of potential sliding,

(ii) Compass and disc-clinometer method and

(iii) Photogrametric method.

These methods call for a rather sophisticated approach and in most local situations, equipment is not available. Nevertheless, simple and crude methods have been devised for estimating the joint roughness coefficient. These include; visual comparisons of surface roughness with the standard set of profiles given in Fig.1, and back-calculation of simple shear tests performed

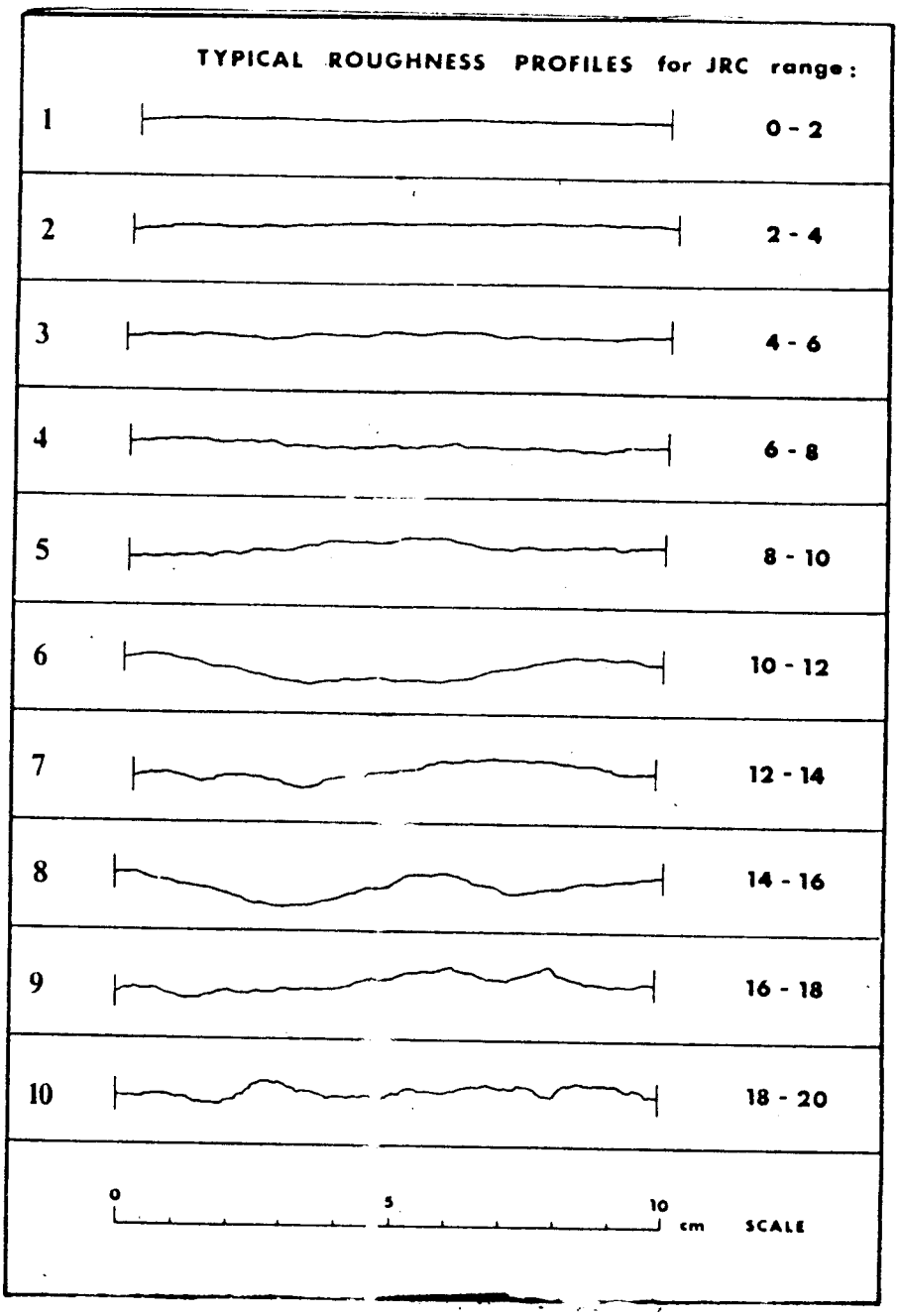

Fig. 1 Standard Roughness Profiles showing the typical range of the Joint Roughness Coefficient (JRC) associated with the discontinuity surfaces [ISRM].

to obtain the basic friction angle of rock (Barton and Choubey 1977). In the later method, equation (2) is rearranged to give:

$$JRC = [\text{Arctan}(\tau/\sigma n)-\phi b]/[\text{Log}(JCS/\sigma n)] \quad ....(4)$$

where all the parameters on the right hand side of equation have been estimated or measured from shear tests.

II. Joint Wall Compressive Strength (JCS)

The measurement of this parameter is of fundamental importance because it is largely the thin layers of rock adjacent to the discontinuity walls that control the strength and deformation properties of the rock mass. JCS is dependent on the degree of weathering of the discontinuity walls.

In the case of unweathered walls JCS is equal to the uniaxial compressive strength (UCS) associated with the rock mass. In a weathered case, the JCS can fall to a mere fraction of the UCS. Since joints are weathered to some extent, in general, JCS is reasonably determined by the Schmidt hammer index test. This is more precise

compared to conventional UCS tests on intact rock cylinders. The reason being that, the thickness of material controlling the shear strength of the discontinuity surface may be as little as a fraction of a millimeter (in smooth-planar joints) to a few millimeters (in weathered,rough-undulating joints). It is the compressive strength of this thin layer of material which is of interest.

Miller (1965) proposed the following correlation between the Schmidt hammer(L-type) rebound number and the joint wall compressive strength:

$$\text{Log JCS} = 0.00088\gamma R + 1.01 \quad \ldots\ldots\ldots\ldots\ldots\ldots (5)$$

where γ = the dry density of rock in KN/m3

R = rebound number between 10 and 60.

A correlation chart is supplied with the instrument on purchase. It makes the work easier because one simply needs to read the rebound number into the chart and read-off the JCS value.

III. Residual Angle of Internal Friction (ϕr)

The residual friction angle represents the

minimum shear strength of a rock discontinuity. It can be measured directly from residual shear tests on carefully sampled rock blocks containing a through-going discontinuity, or can be determined indirectly from Richards'(1975) empirical relationship. In the later case the empirical relation is as follows:

$$\phi r = (\phi b - 20) + 20(r/R) \quad \text{.....(6)}$$

where ϕb = the basic friction angle of rock

r = Schmidt hammer rebound number on weathered discontinuity surfaces

R = Schmidt hammer rebound number on unweathered rock surfaces.

The basic friction angle can be obtained from conventional shear tests performed on rock core with test ends sawn flat.

3.2.3 Practical Application of the Empirical Relation

Equation (3) can be used in three different ways:

(i) curve fitting to experimental peak shear strength data,

(ii) extrapolation of experimental peak shear strength data, and

(iii) prediction of the peak shear strength.

The families of peak shear strength envelopes shown in Fig.2, illustrate the practical nature of this empirical law of friction. Values of JRC of 20, 10 and 5 have been used to illustrate the effect of joint roughness. The curves numbering 5, 10, 50 and 100 (in units of MN/m2) illustrate the effect of the joint wall compressive strength JCS.

Barton (1971a) developed a log-tan chart (Fig.3) for the empirical relation, equation (2). Using this chart; curve fitting, extrapolation and prediction of peak shear strength data can easily be done. For example, Fig.3 shows a curve fitted to the experimental shear strength data for a rock joint with JRC of 20 and ϕb of 30 degrees. The ratio $\tau peak/\sigma n$ is on the abscissa with a tangent scale and $\sigma c/\sigma n$ is on the ordinate with a log scale. σc is the uniaxial compressive strength (UCS) of the rock which is equivalent to the JCS of an unweathered discontinuity.

Following Hoek (1970), Barton (1972) adopted a simplified distribution of normal stress along a plane of failure behind the slope. This was proposed in the following equation:

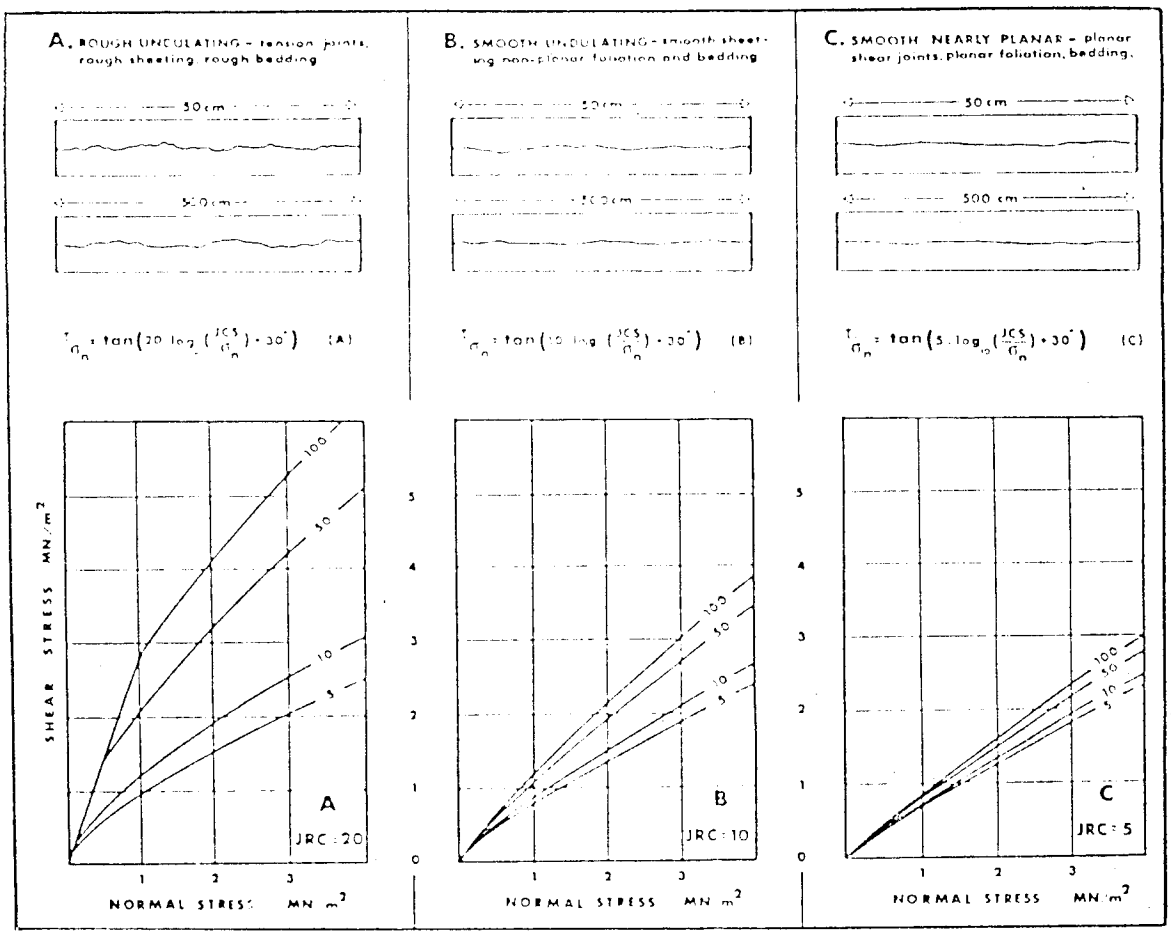

Fig. 2 Empirical Law of Friction in graphical form. Eac curve is numbered with the appropriate JCS value (units o MN/m2). The roughness profiles are intended as a approximate guide to the appropriate JRC values 20, 10 an 5. Completely smooth discontinuities have JRC = 0 [afte Barton and Choubey,1977].

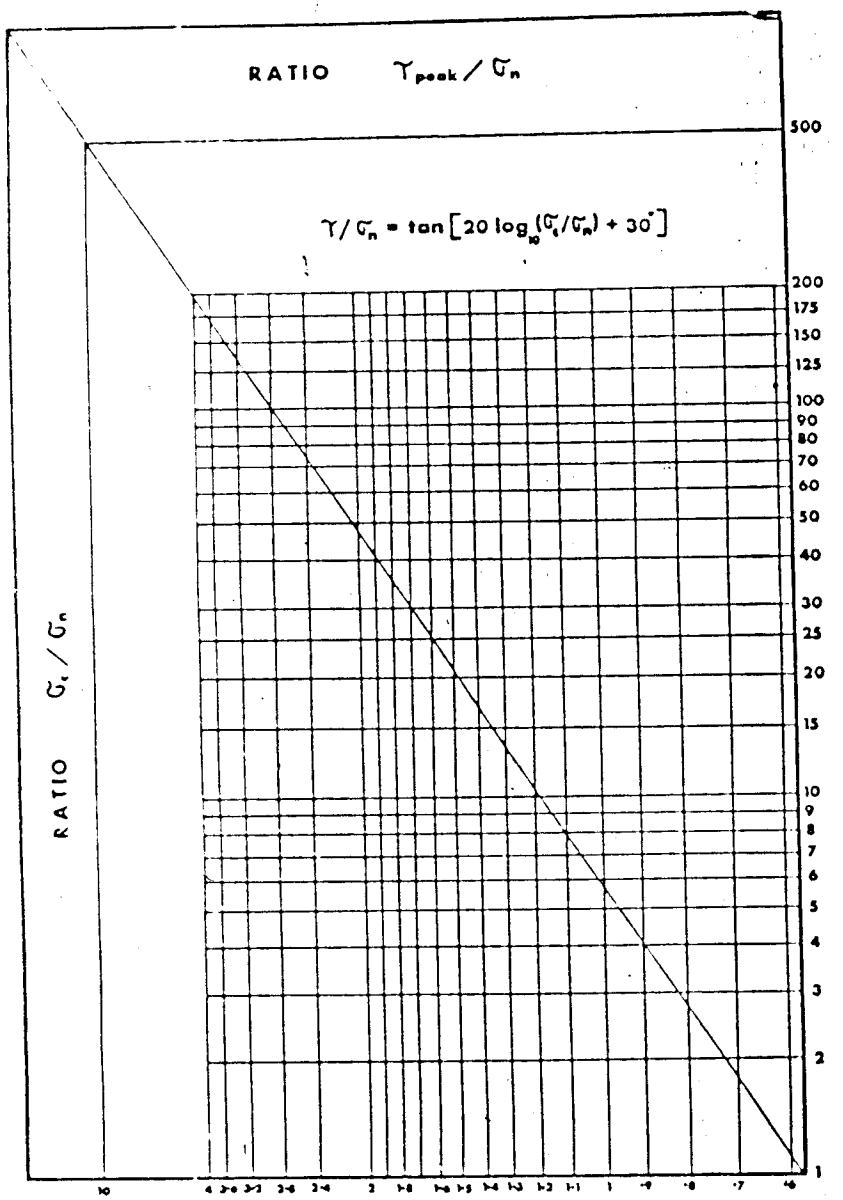

Fig. 3 A Peak Shear Strength Criterion for rough-undulating Rock Joints [after Barton,1971a].

$$Gn = \gamma H(\cot\beta - \cot\psi)\sin\beta.\cos\beta \quad \ldots\ldots\ldots\ldots(7)$$

where γ = rock mass density (KN/m3)

H = height of slope (m)

β = mean inclination of failure plane

ψ = overall slope angle.

This equation can be used to estimate and predict the range of normal stress in a given slope problem as indicated in Fig.4.

3.3 Other Rock Strength Tests

3.3.1 The Point Load Index Test

This index test is used in providing quick quantitative rock strength data for rock strength classification. The results obtained from this test are in form of strength indexes (Is). The test is usually performed on rock core or on unprepared pieces of rock. The strength index,Is, is defined by the equation:

$$Is = P/D^2 \quad \ldots\ldots\ldots\ldots\ldots\ldots\ldots\ldots\ldots\ldots(8)$$

where P = the load in KN at failure

D = the distance between loading points which is equivalent to the specimen diameter.

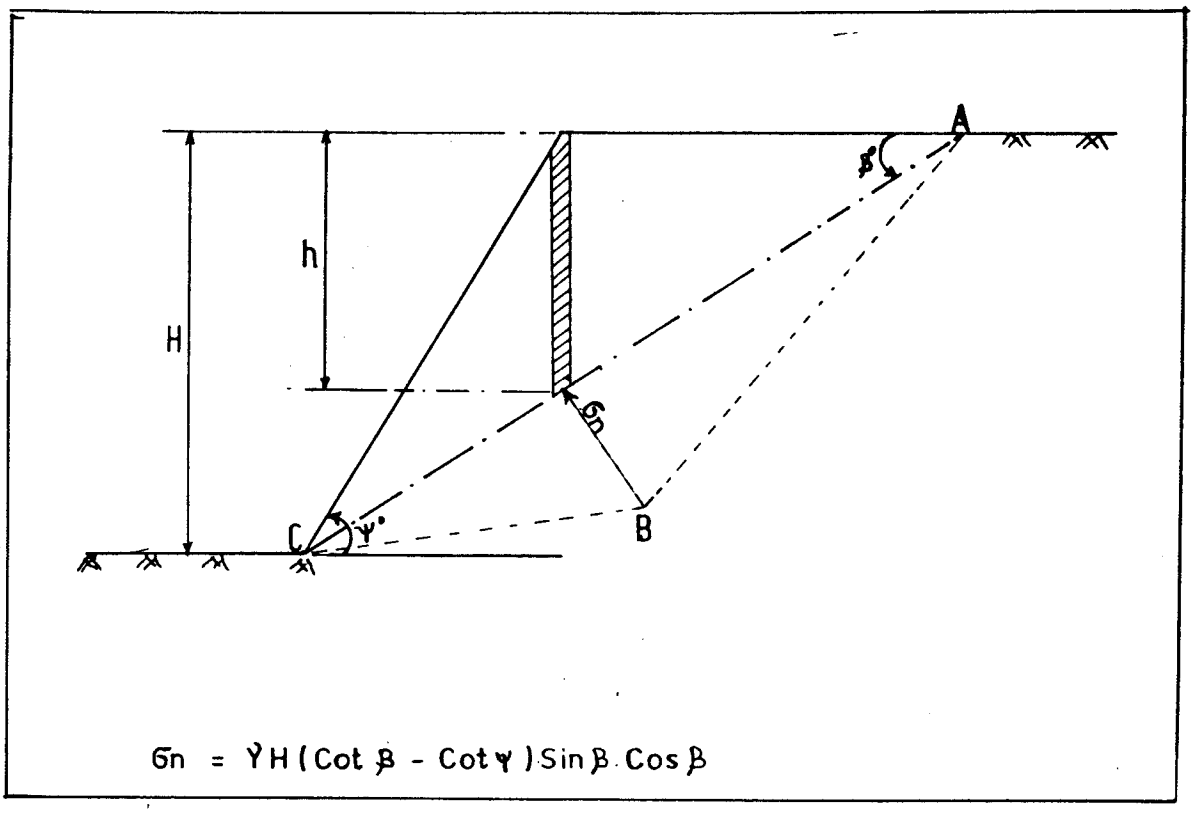

Fig. 4 A Simplified distribution of Normal Stress along a plane of failure in a jointed and drained Rock Slope [after Hoek,1970].

The strength index, in itself, is not applicable in any problem solving equation. Reasonable correlation between the point load index (Is) and the more useful uniaxial compressive strength (UCS) of rock has, however, been worked out. Bieniawski (1974) showed the following relationship between the two strength parameters, for tests conducted on rock core:

$$UCS = k(Is) \quad \ldots\ldots\ldots\ldots\ldots\ldots\ldots\ldots\ldots\ldots (9)$$

where k = the compressive strength to index ratio corresponding to core size.

This was shown to yield values of **k** of 18, 21 and 24 corresponding to core sizes EX(21.5 mm), BX(42 mm) and NX(54 mm) respectively (Fig.5).

3.3.2 The Shear Box Test

The direct shear box test is widely used in obtaining shear strength parameters in rock. The cohesion 'c' and the friction angle 'ϕ' are usually obtained from this test. The test is conducted on pairs of carefully sampled rock blocks or core, containing a through-going discontinuity, so that the shear strength results obtained can be related to the same discontinuity planes.

Fig. 5 Relationship between Point Load Index and Uniaxial Compressive Strength for Different Core Sizes. [after Bieniawski, 1974].

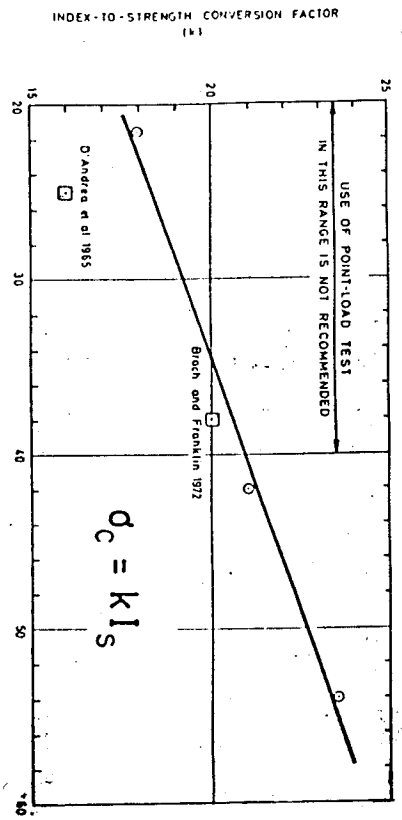

(a) Size correlation graph for index-to-strength conversion.

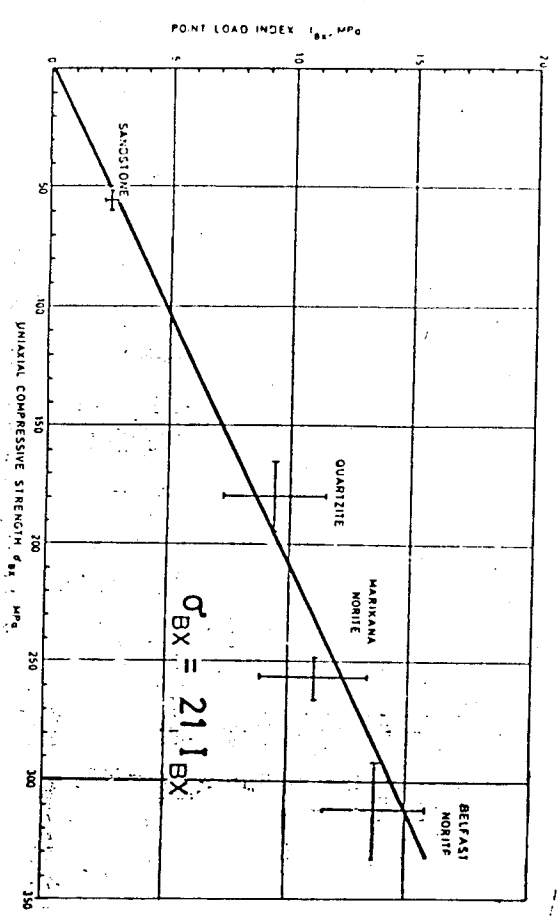

(c) Relationship between point-load index and uniaxial compressive strength for BX core (42 mm).

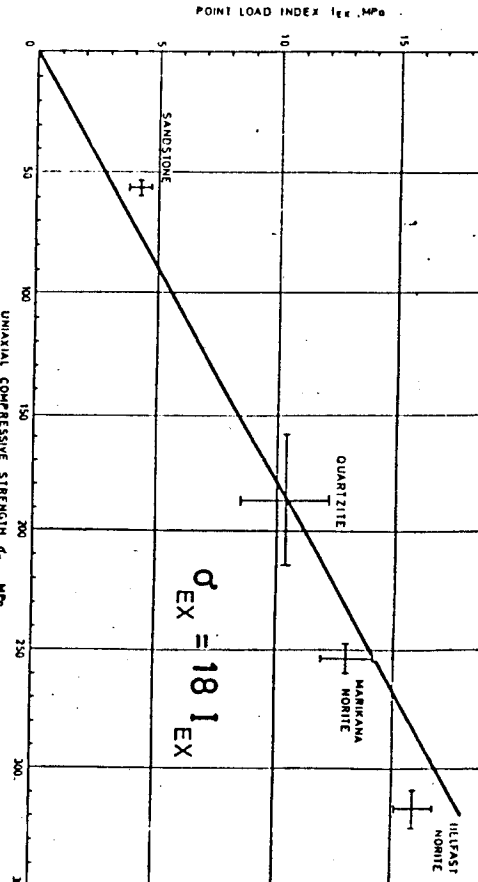

(b) Relationship between point-load index and uniaxial compressive strength for EX core (21.5 mm).

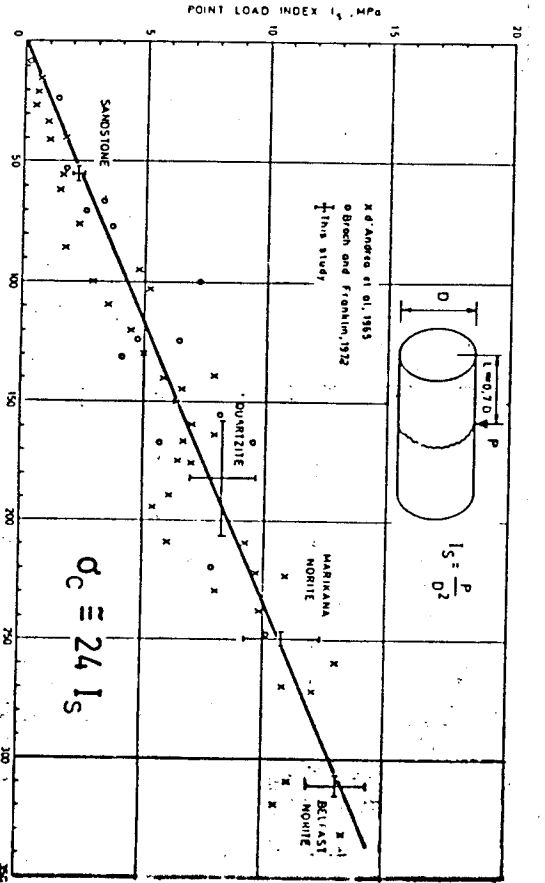

(d) Relationship between point-load index and uniaxial compressive strength for NX core (54 mm).

Though reasonably easy to perform, there is a problem of achieving a uniform stress distribution in the shear-box. It has been recognised also that, because there is no uniformity in the construction of the machines in use around the world, the results of one worker may differ with the results of another even though identical specimens were tested (Goodman 1970). Because of the importance of the test more elaborate shear machines have been developed. Some of the examples are; Hoek and Pentz Direct Shear Machine at Imperial College, Deere and Coulson Direct Shear Machine at University of Illinois and SEIL Direct Shear Machine in Paris.

Chapter 4

The Structural Setting and Geology of the Nchanga Open Pit

4.1 General

Exploration work as early as the 1920s revealed copper mineralisation in three horizons of the rock formations in the Nchanga area. The near surface horizon averaging 30 metres thick was called 'Nchanga ore-body', renamed Upper ore-body (UOB); the intermediate one averaging 6 metres thick was named the Intermediate ore-body (IOB); and the bottom one averaging 20 metres thick was named the Lower ore-body (LOB).

Mining of the lower ore-body (LOB), by underground methods, started in 1928. Attempts to mine the upper ore-body (UOB) in the same manner were unsuccessful due to the weak and wet nature of both the footwall and hangingwall rock formations. It was not until 1955 when open pit mining methods were considered for this ore-body. Subsequently the Nchanga Open Pit was started.

At present Nchanga Open Pit ranks as one of the largest open cast copper mines in the world. Though originally designed to mine the upper ore-body only, both the intermediate and lower ore-bodies are also being mined. Measuring 3,600 metres in length, 1,500 metres in width and over 300 metres to the sump, its present production

target is 300,000 tons of ore at more than 2.5% T.Cu grade per month. Electric crawler shovels, rotary drill masters, 100ton-dump trucks and scrapers constitute a production fleet.

For the purpose of planning and design, the pit is divided into section lines running near perpendicular to both faces along strike at 120-metre intervals. They are numbered from west to east in a numerically increasing order. The western extent of the pit has been mined above underground workings (Fig.6).

4.2 Geology

The rocks at Nchanga consist of a clearly defined sequence of sedimentary rocks and as at other mines on the Zambian copperbelt, the ore horizons occur within the Lower Roan Group of the Katanga System. The material forming the bulk of the overburden is designated the Upper Roan Group (Fig.7).

For the purpose of simplicity, the sedimentary sequence of the Upper Roan Group is subdivided into five main stratigraphical formations following a local nomenclature, and these are:

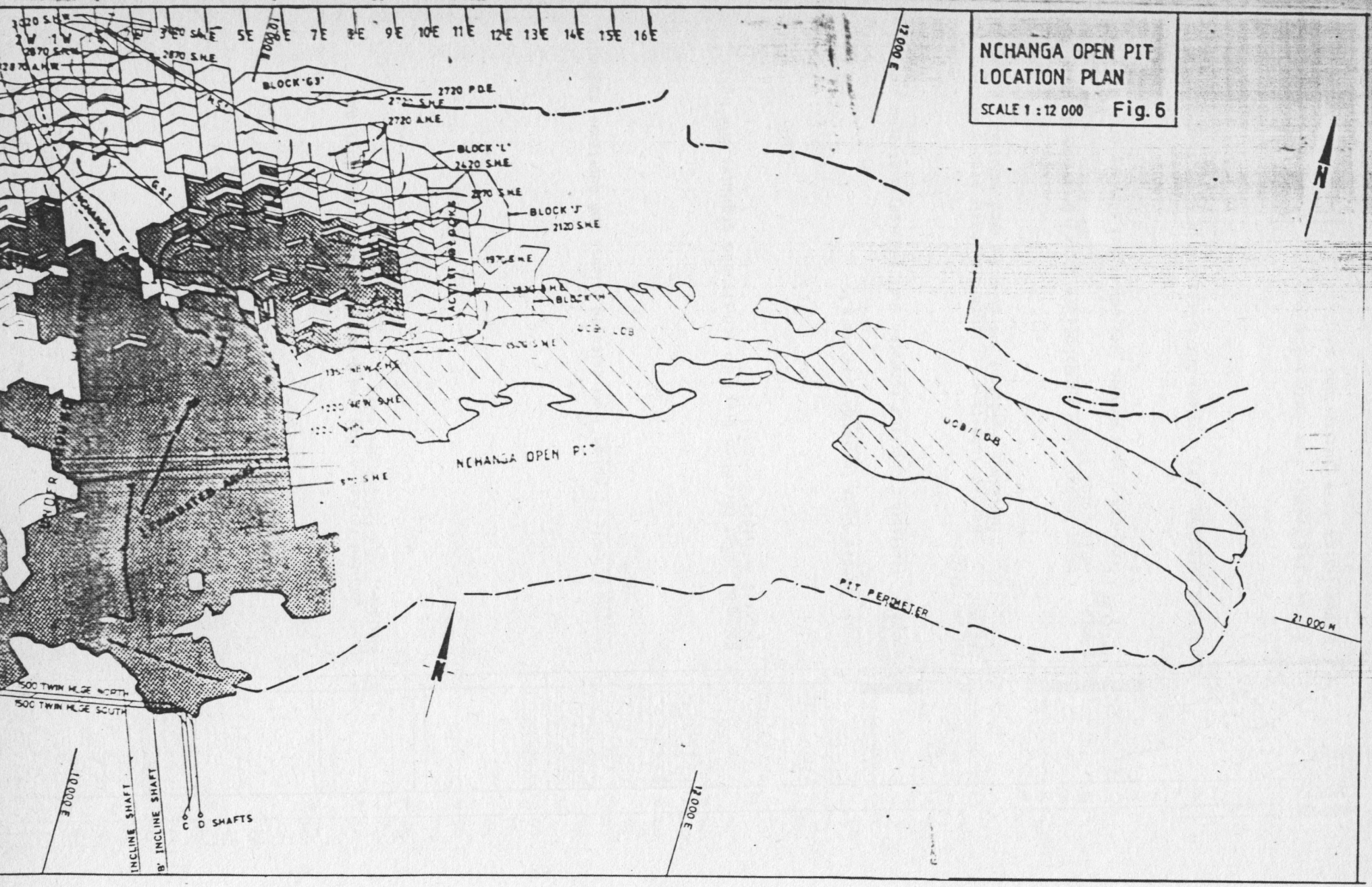
NCHANGA OPEN PIT
LOCATION PLAN
SCALE 1 : 12 000 Fig. 6
BLOCK 'G3'
BLOCK 'L'
BLOCK 'J'
2720 PDE
2720 AME
2670 SME
2870 SME
2120 SME
NCHANGA OPEN PIT
UCB/LOB
PIT PERIMETER
21 000 N
1500 TWIN HOLE NORTH
1500 TWIN HOLE SOUTH
INCLINE SHAFT
'B' INCLINE SHAFT
C D SHAFTS
12 000 E
3 000 E
N

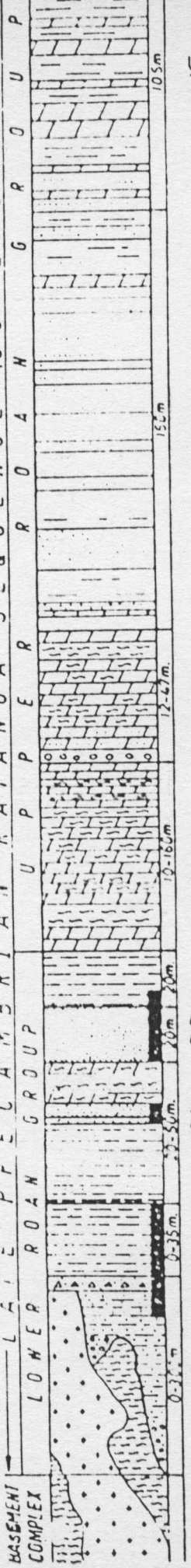

Upper Roan Dolomites Formation: Varicoloured siltstones and talcose dolomites.

Shale with Grit Formation Grey and green gritty, sandy argillites and siltstones, some talcose dolomites

Chingola Dolomite Formation: Light coloured, talcose and quartzose dolomites.

Dolomitic Schist Formation: Grey mica schists and argillites with light coloured schistose dolomites

Upper Banded Shale Formation: Grey shale.

UPPER OREBODY Feldspathic Quartzite Formation: Buff coloured, feldspathic arenite.

INTERMEDIATE OREBODY Banded Sandstone Formation: Grey, finely bedded siltstones and feldspathic sandstone and dolomitic mica schists.

LOWER OREBODY Lower Banded Shale Formation ('Ore Shale'): Grey and black carbonaceous shale

Transition Arkose member: Grey, calcareous siltstone breccia.

Arkose Formation: Grey, conglomeratic arkose and lithic greywacke.

Fig. 7

Nchanga Red Granite: Pink microcline granite.

Lufubu System: Grey gneisses and schists.

(i) Upper Roan Dolomites (URD) - mostly lateritic to clayey transported soils;

(ii) Shale With Grit (SWG) - predominantly an argillaceous succession of weak to very strong bands of argillites, greyish pink to purple in colour, with zones of gritty fine to medium grained sandstones;

(iii) Chingola Dolomite (C/DOL) - a predominantly weak horizon of light coloured quartzose and talcose dolomites with cherty residues;

(iv) Dolomitic Schist (DOLSCH) - a competent alternating sequence of micaceous quartzose dolomites and dolomitic mica-schists interbedded with argillites;

(v) Upper Banded Shales (UBS) - grey laminated and finely bedded phyllitic shales with dolomitic cementation in places.

The Lower Roan Group is also subdivided into another five main rock formations, going down the succession, as follows:

(vi) The Feldspathic Quartzites (TFQ) - dark grey to light coloured glassy quartzites with argillitic bands, and generally mineralised (UOB);

(vii) Banded Sandstones (BSS) - composed of thinly bedded feldspathic sandstones and siltstones with micaceous quartzites. It occurs as an 'upper' and 'lower' band seperated by a mineralised thin band of the Pink Quartzite constituting the IOB;

(viii) Lower Banded Shale (LBS) - a predominantly black, carbonaceous, laminated dolomitic shale; sometimes a grey, silty argillite to a finely laminated quartzite, generally mineralised and forms whole or part of the LOB;

(ix) Arkose (ARK) - a medium to coarse lithic greywacke of quartz microline and sericite;

(x) Nchanga Red Granite (GRAN) - a pink microline granite known as the basement conglomerate.

4.3 Major Structural Features

The main structural feature in the location of Nchanga Open Pit is, what is known as, the Nchanga Syncline. Its surface trace stretches 12 kilometres long and is about 3 kilometres wide. It, generally, strikes east of south-east and north of north-west (Fig.3). The most striking feature about the syncline is that its two limbs (the south and north limbs) dip asymmetrically towards the synclinal axis, differing greatly between

their respective dip angles. The southern limb, on which the open pit is situated, dips gently at an angle averaging between 30 and 35 degrees while its northern limb dips steeply to near vertical in most cases (Fig.9).

Other structural features are faults, folds and bedding planes. However, faulting is not prominent within the location of the pit apart from the main Nchanga Fault which cuts across the western extent of the pit as shown in Fig.8. Within the southern limb of the Nchanga Syncline, the uncomformable localised folding between the Upper Roan and Lower Roan formations is interesting. Folding in the Upper Roan Group bears no relation to that of the Lower Roan. Fold structures in the Upper Roan Group are generally open and symmetrical while those in the Lower Roan Group are asymmetrical and sometimes recumbent and only confined to TFQ and BSS formations. Little or no folding of the underlying Lower Banded Shale and Arkose units has taken place (Fig.9).

4.4 Weathering Effects

Pervasive weathering has affected the properties of the Chingola Dolomite and the Banded Sandstones to a

significant degree. Even in sections where the Chingola Dolomite appears to be less weathered, for example between section lines 6E and 9E of the hangingwall, it retains an upper highly weathered schistose contact with the Shale With Grit . Other formations exist as fairly weathered over a greater extent along strike, except in the western portion of the pit where weathering has been aggravated by the influence of the underground caving.

GENERAL GEOLOGICAL PLAN AND TOP OF BASEMENT CONTOURS OF THE NCHANGA SYNCLINE AREA

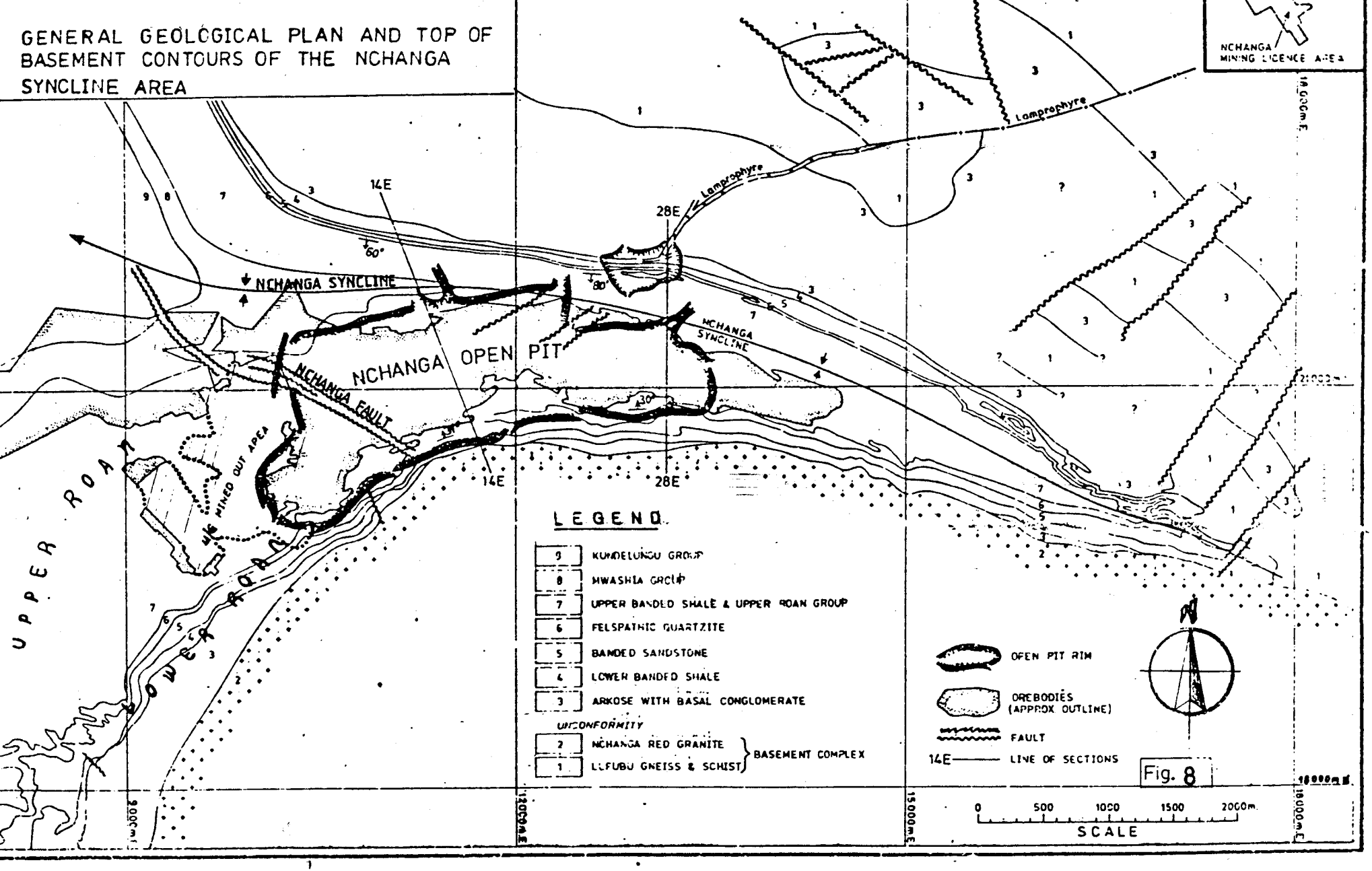

Fig. 8

IDEALISED SECTION THROUGH THE NCHANGA SYNCLINE

Scale 1 : 5000 FIG. 9

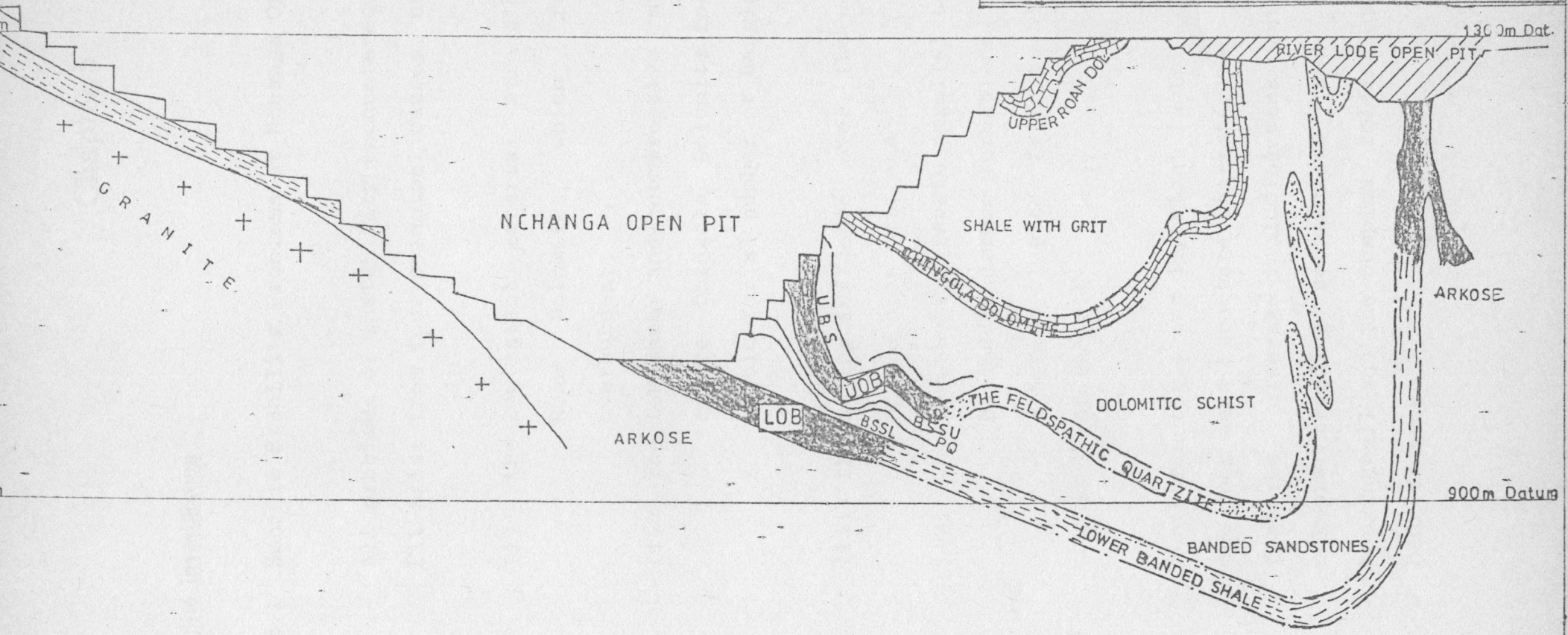

Chapter 5

Site Investigation

5.1 Secific Stability Problems at Nchanga Open Pit

All problems of instability encountered at Nchanga Open Pit arise from four principal causes, namely:

(i) the low intact material strength of the Upper Roan Dolomites which form the soft overburden;

(ii) the low shear and compressive strength of the entire Chingola Dolomite formation, responsible for a number of hangingwall failures;

(iii) the caving influence over the western extension of the open pit; and

(iv) the low shear strength parallel to bedding of the Banded Sandstone formations, responsible for a series of plane failures along the footwall of the pit.

Another notable and important factor of instability is the rock mass structure characterised by the bedding features, cleavage including weak contact zones, joint network trending subparallel and normal to the hangingwall and the complex folding patterns of the beds of rock.

5.1.1 Intact Material Strength of the Upper Roan Dolomites

The strength of the Upper Roan Dolomites has less influence on the stability of the overall pit slopes. However, in sections where the material is thick, it influences the design and layout of the crest area. Analytically, the material is considered to behave isotropically and it is, therefore, treated as a soil.

5.1.2 Shear Strength of the Chingola Dolomite

The shear strength properties of the Chingola Dolomite are complex due to variable weathering and the presence of talcose and micaceous components . It exists as decomposed material over much of its strike length and down dip. However, between section lines 7E and 9E the formation exists as a competent and intact rock. Typical shear strength values determined from routine laboratory tests, and usually applied in stability calculations, range between 10 - 20 KPa and 15 - 25 degrees for the cohesion and friction angle, respectively.

The presence of this weak unit at almost half way down the pit's hangingwall, has adversely affected the stability of the relatively competent Shale with Grit overlying it. Because it is highly compressible, it tends to extrude under load when exposed. Most of the deep seated failures, that have occured across the pit's hangingwall, have toed in the Chingola Dolomite. One example of such failures is shown on Plate No.5, and presented on plan and section in Figs.10 and 11, respectively. The failure demonstrates a case of cutting through intact rock. The low tensile strength associated with Shale with Grit (due to cleavage) makes it possible for such a failure to occur. Tensile strength tests conducted on Shale with Grit samples have yielded values between 0.2 MPa and 1.0 MPa (Dalgleish,1978).

5.1.3 Influence of Caving

Underground block caving of the lower ore-body between section lines 1E and 8E has, inevitably, influenced large cave cracks and differential subsidence of ground in the north-west corner of the open pit. The caving of ground in the undergrond workings immediately below the open

pit is considered to have contributed to the recurring slope failures of the pit's north-western corner. Indicated on Fig.12 are the deep seated cracks prior to the December 1984 slope failure, which is included on fold-out plan, Fig.13. (See Plate No.6 also) The influence of caving can also be seen in the altered geological fabric of the rock formations in the zone, especially those of the Upper Roan Group. Recent studies of caving characteristics made on the basis of subsidence observations (Steffen, Robertson and Kirsten Report No. MI1813/5 Oct.1981) have helped to examine the potential effects of caving on the final slopes, and to assess the effect of caving/subsidence on the strength of rocks. Though no comprehensive studies have been conducted to establish accurate behavioural models, it has been recognised that there is a gradual reduction in the material intact strength towards the cave (Steffen, Robertson and Kirsten Report No. MI1042/23 Aug.1984).

5.1.4 Shear Strength of the Banded Sandstones

Banded Sandstones, generally, exist as an incoherent formation with low compressive and

tensile strengths. Low cohesive strength 'c' ranging from 10 to 50 KPa, and friction angle 'ϕ' ranging from 25 to 30 degrees have been obtained from routine laboratory tests. This formation has been responsible for the lot of plane failures along the pit's footwall, where it dips into the pit. Indicated on the fold-out plan, Fig.13, are some of the major failures attributed to the BSS formation. However, its influence on the hangingwall slopes, where it dips away from the pit, is yet to be seen though it has been exposed over a considerable strike length, for some time now.

5.2 Intact Material strength

The rocks at Nchanga can, conveniently, be grouped into two classes with respect to rock mass strength as follows:

a) Class I Rocks - whose stability is controlled by the intact material strength. Included in this class are; Upper Roan Dolomites, Chingola Dolomite and Banded Sandstones.

b) Class II Rocks - whose stability is controlled by the rock mass structure, and these are; Shale With Grit, Dolomitic Schist, Upper Banded and Lower Banded Shales.

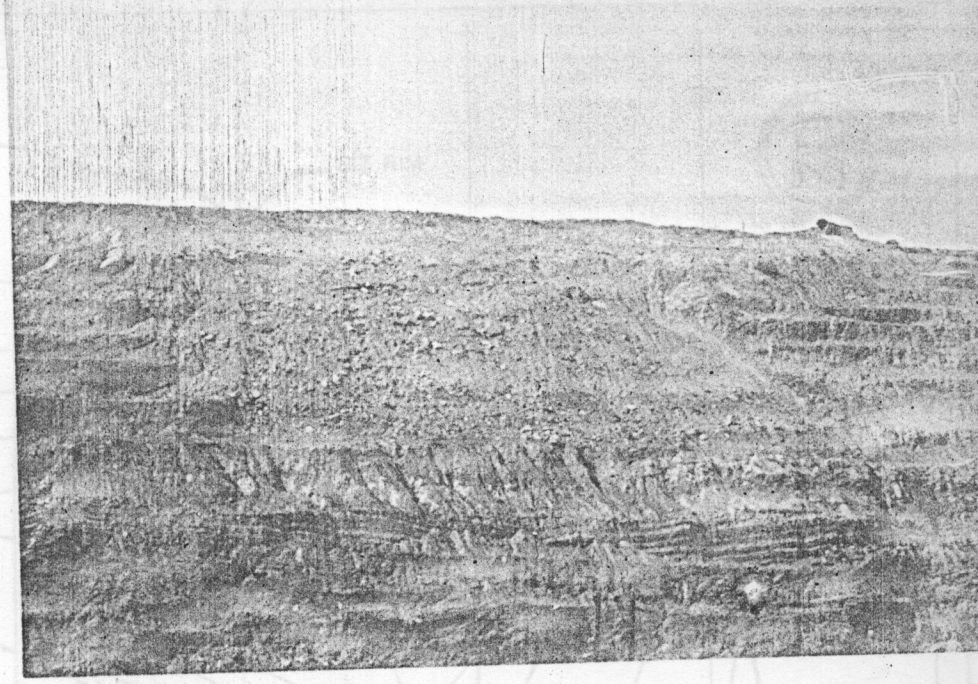

Plate 5: Hangingwall failure at Nchanga O/Pit (Apr. 1983) in the SWG formation. Failure was influenced by the underlying soft C/Dolomite formation. About 1.5 million bcm of material were involved compelling a readjustment to the original design cut.

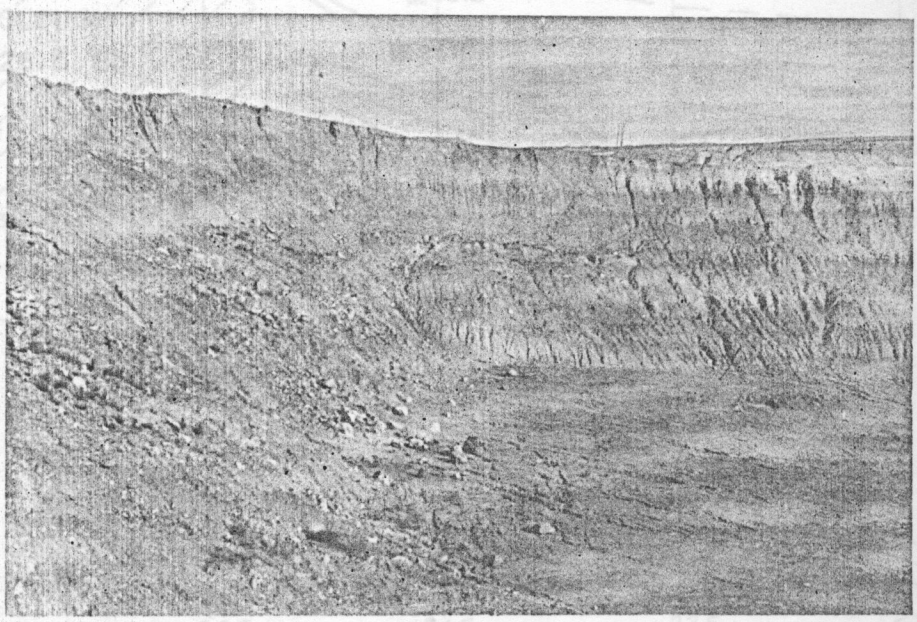

Plate 6: Circular failure at the north - western corner of NOP in the Upper Roan Dolomite formation (Dec. 1984); influenced by underground caving and a high water table behind the slope. More than 2.5 million bcm of material were brought down and production was affected.

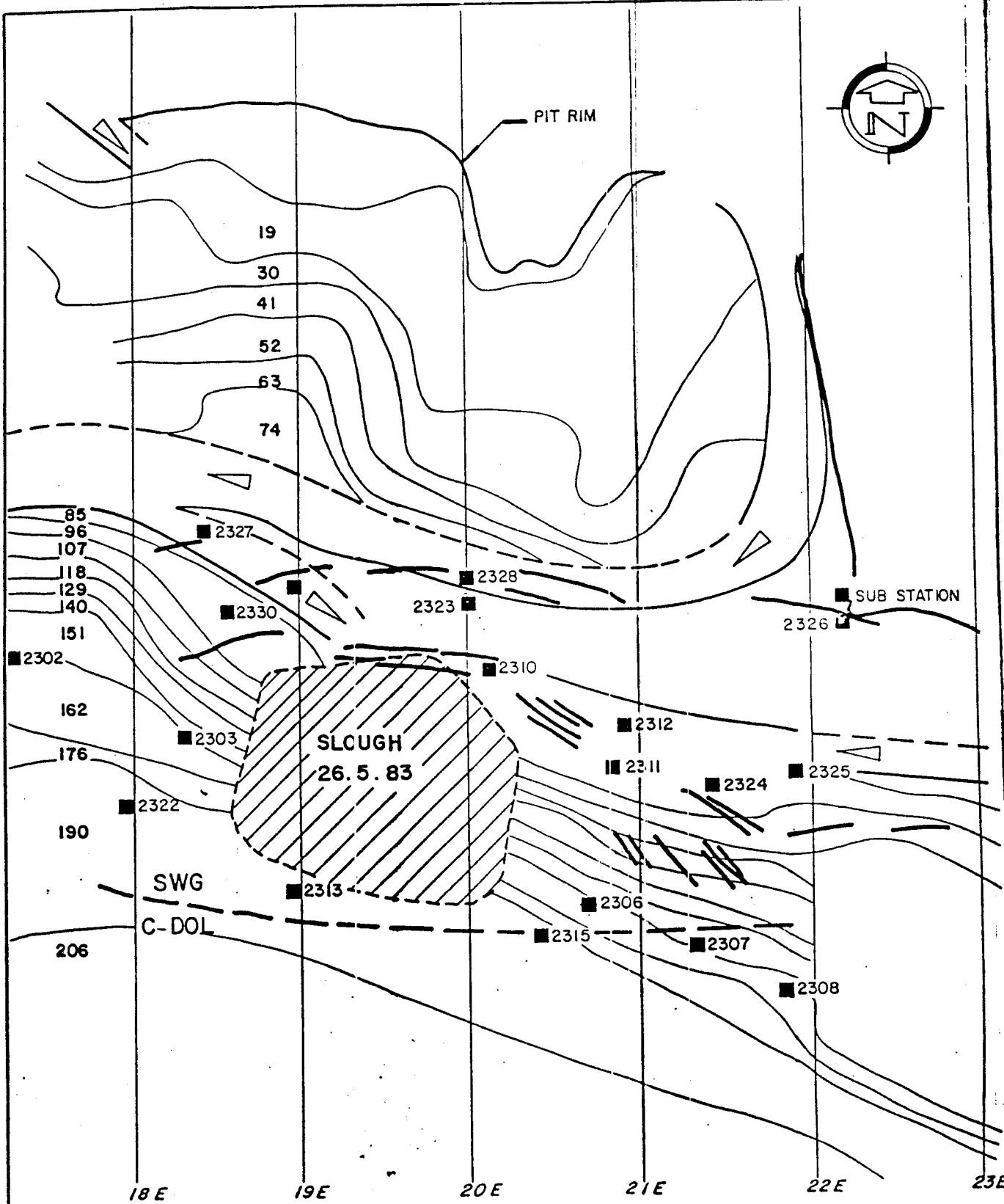

PLAN SHOWING NORTH FACE SLOUGH AND ASSOCIATED CRACKING

SCALE		NCHANGA - STABILITY OF 371 CUT	FIG Nº
1:4000			10

SCALE 1:2000

NCHANGA-STABILITY OF 371 CUT

FIG 11

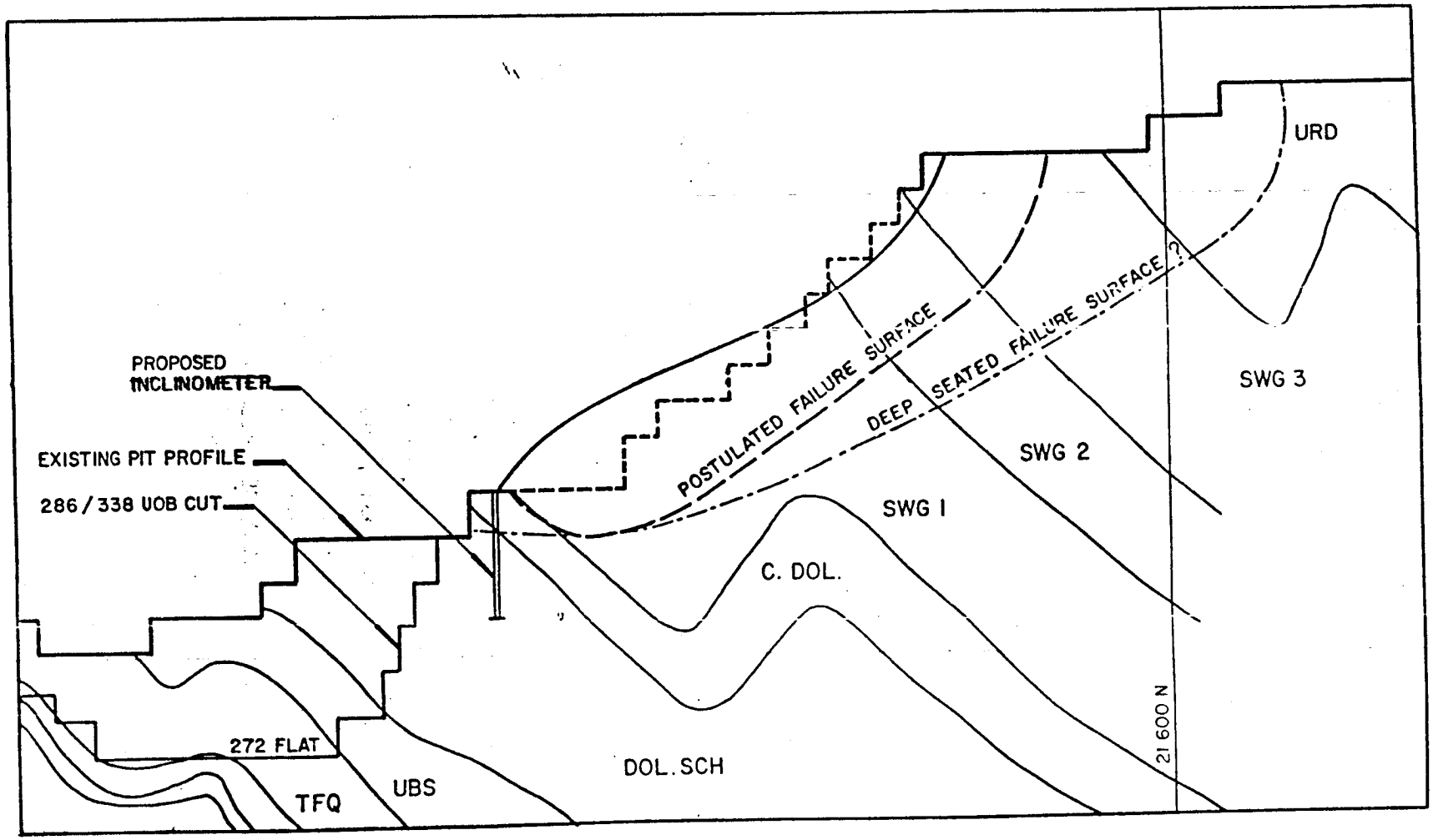

SECTION 20 E. PROPOSED 286/338 UOB CUT SHOWING POSSIBLE MODE OF FAILURE

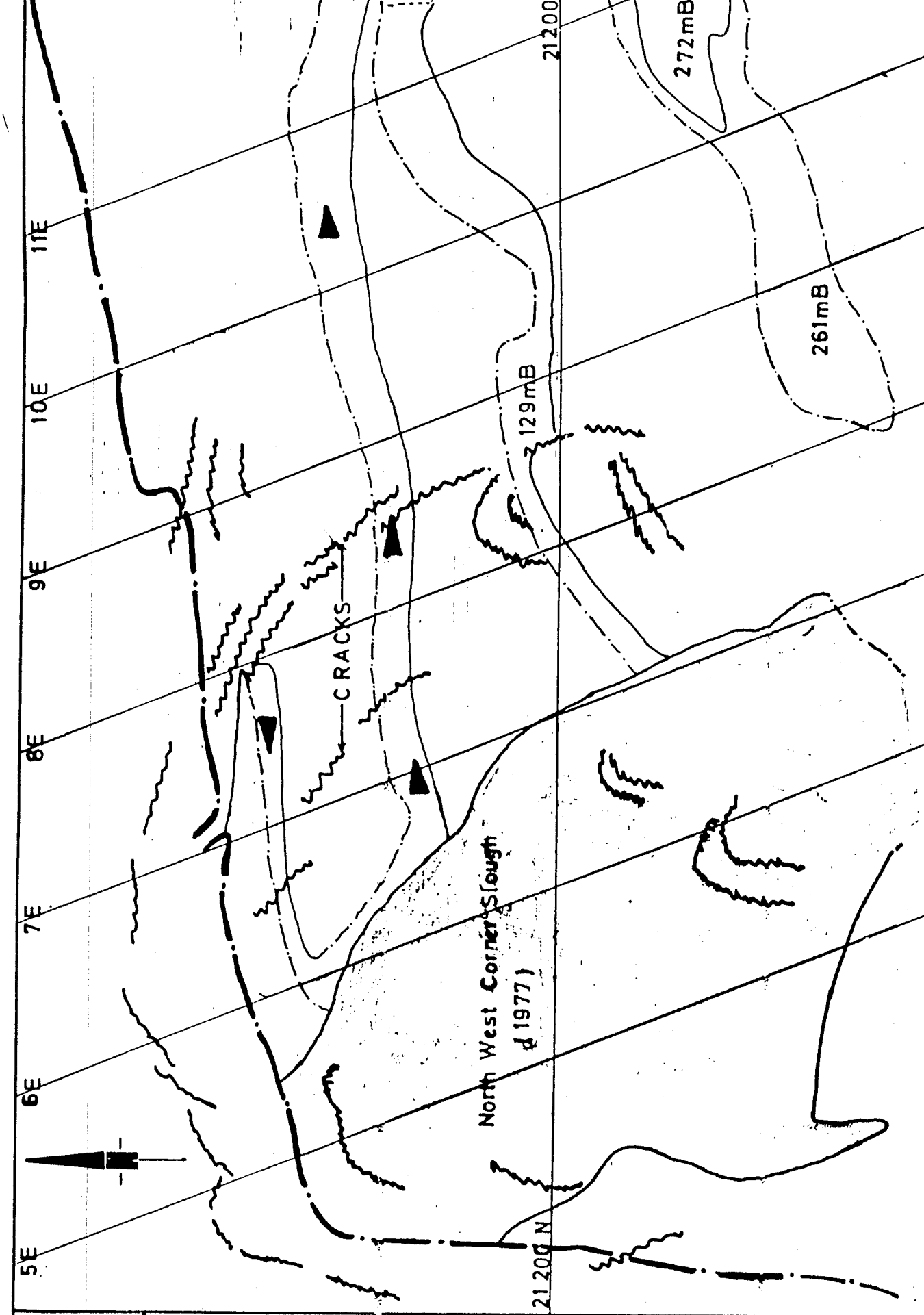

Scale 1 : 4000	PLAN SHOWING CRACKING IN NORTH WEST CORNER	Fig. 12

The Class I rocks are treated as soils and are thus amenable to testing using soil strength testing techniques. The Class II rocks are treated under rock testing and rock mass classification techniques.

5.3 Rock Mass Deformabilty

Typical ranges of rock mass deformability for the various Nchanga rocks are given in Table 1. The estimates were obtained from small scale laboratory tests and rock mass classification studies.

5.4 Rock Mass Structure

The complex geology and structure associated with the Nchanga Syncline has resulted in a complex pattern of jointing which varies from lithology to lithology as well as within a single unit. Piteau (1970) described in detail the joint patterns obtaining in the various lithological units at Nchanga. With reference to the hangingwall slope, joint surveys have usually been confined to the Shale With Grit and Dolomitic Schist horizons. Occassionally, surveys have been extended to the Upper Banded Shale and The Feldspathic Quartzite formations (Figs.14 and 15).

Table 1 Rock mass Deformability Estimates

ROCK TYPE	MODULUS OF DEFORMABILITY (GPa)
SHALE WITH GRIT	15 - 25
CHINGOLA DOLOMITE (decomposed)	0.1 - 5
" " (mod. weathered)	5 - 10
" " (unweathered)	10 - 20
DOLOMITIC SCHIST	20 - 30
UPPER BANDED SHALE (weathered)	1 - 5
" " " (unweathered)	15 - 25
THE FELDSPATHIC QUARTZITE	25 - 35
BANDED SANDSTONES	5 - 10
LOWER BANDED SHALE	15 - 25
ARKOSE	25 - 40

(Steffen, Robertson & Kirsten Report No. MI1042/23 Aug.1984)

EQUAL AREA, LOWER HEMISPHERE, POLAR PROJECTION

CONTOUR PLOT

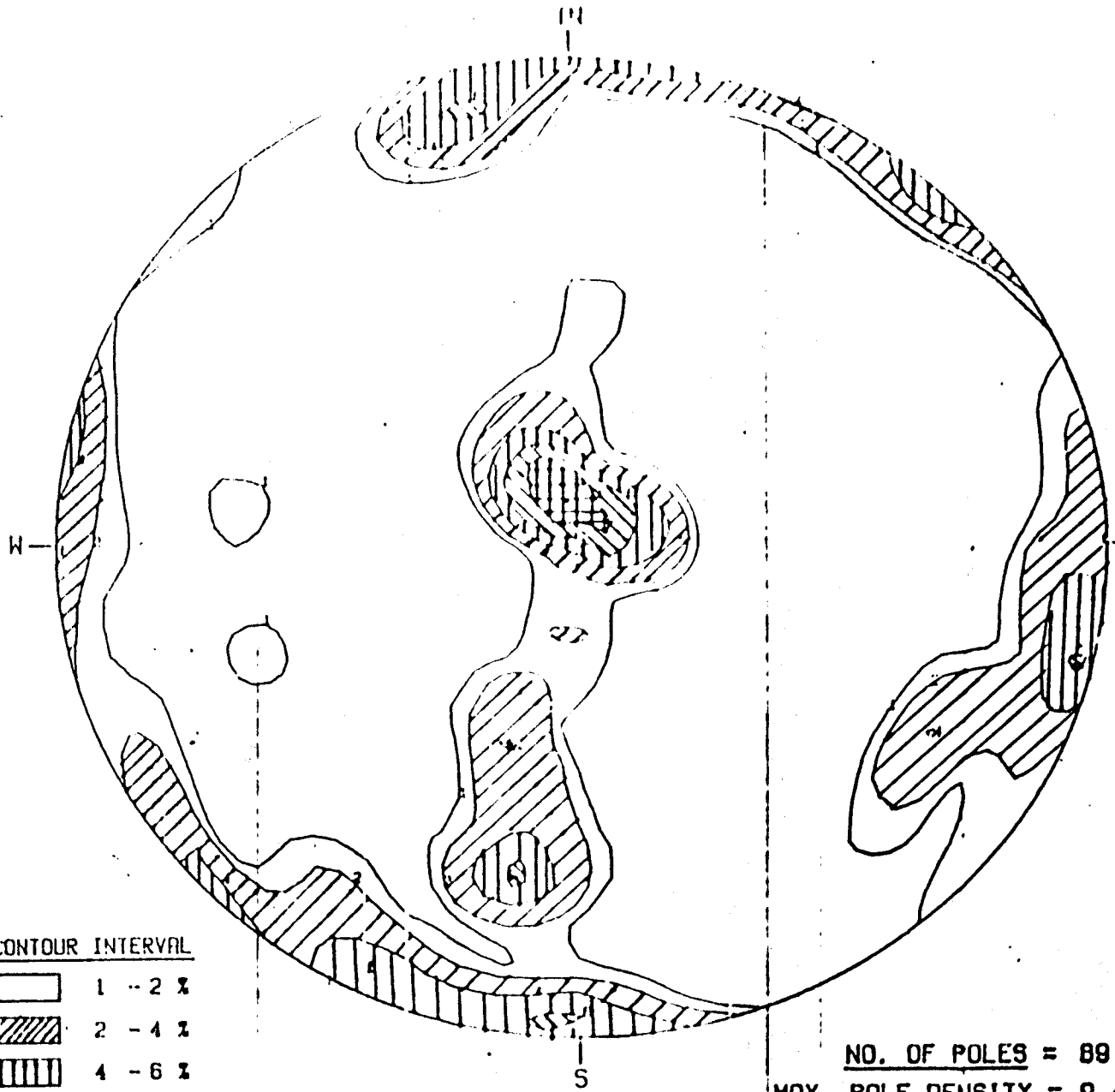

CONTOUR INTERVAL

	1 - 2 %
	2 - 4 %
	4 - 6 %
	6 - 8 %
	> 8 %

NO. OF POLES = 89

MAX. POLE DENSITY = 8.4

PLOT OF ALL JOINTS MEASURED IN THE SHALE WITH GRITS FOR ROCK MASS CLASSIFICATION

	NCHANGA OPEN PIT	FIG. NO. 14

FIGURE - TRUE DIP-DIP DIRECTION ; POLAR PROJECTION

CONTOUR PLOT

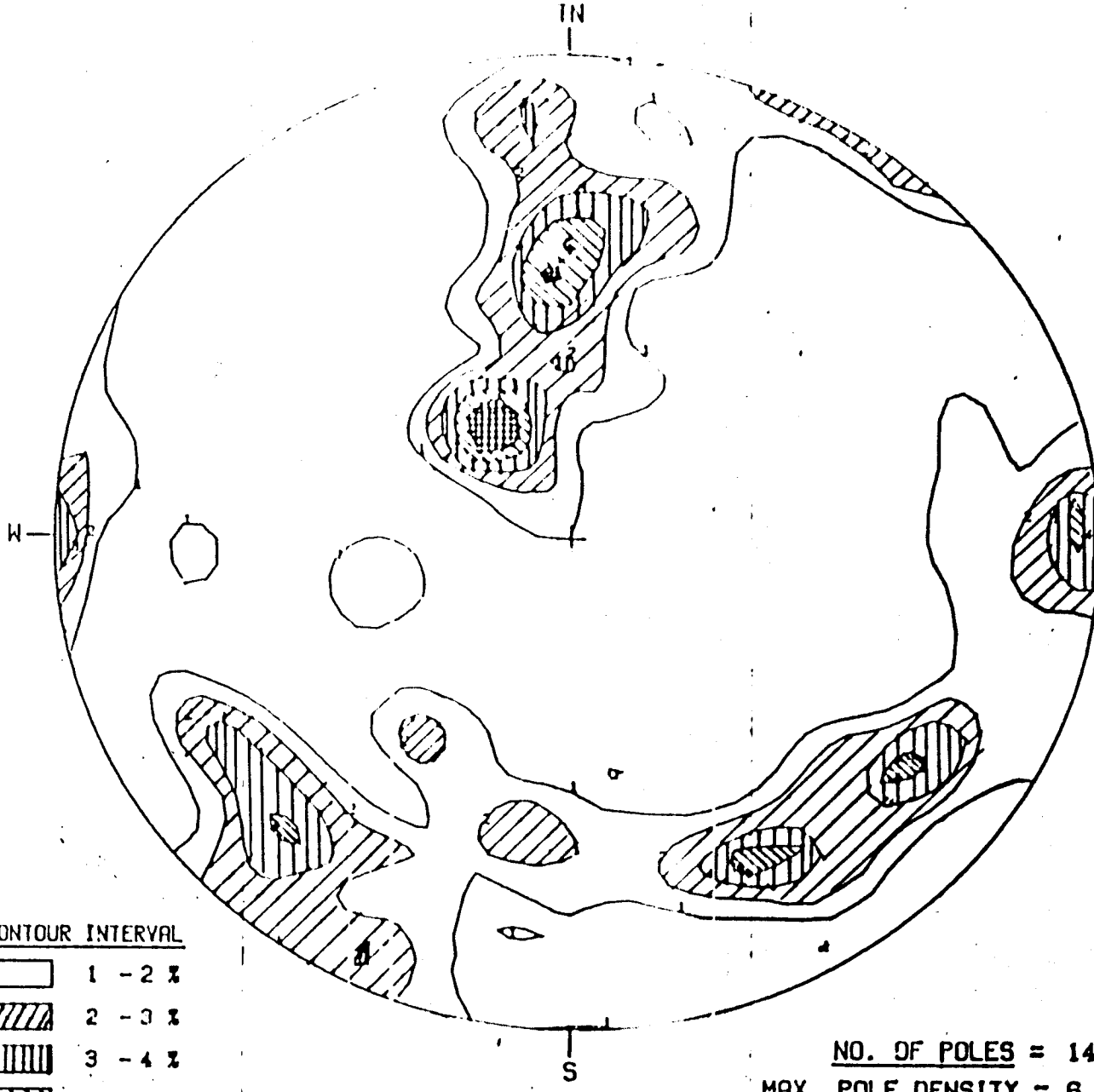

CONTOUR INTERVAL

	1 - 2 %
	2 - 3 %
	3 - 4 %
	4 - 5 %
	> 5 %

NO. OF POLES = 14

MAX. POLE DENSITY = 6.

PLOT OF JOINTS MEASURED IN THE TFQ, UBS AND UUL SCHISTS FOR THE ROCK MASS CLASSIFICATION

	NCHANGA OPEN PIT	FIG. NO. 15

Of particular concern to slope stability, is the orientation of the joints in relation to the slope face. From experience, the majority of stability problems encountered at Nchanga Open Pit arise from an interaction between adversely dipping bedding planes, on one hand, and a set of joints including cleavage, on the other. Blasting effects have also added to the intensity of the joint action through the propagation of fresh cracks and widening of existing planes of weakness.

For the purpose of this work, all discontinuities occuring from natural processes, such as; bedding planes, cleavage, joints, minor faults etc. are classified under Type 1. All the artificially induced fractures, causing a break through intact material, such as tension cracks resulting from excavating and blasting operations, are classified under Type 2.

5.5 Influence of Rock Discontinuities on Slope Stability at Nchanga Open Pit

As already mentioned in section 2.2, failures in rock slopes are largely controlled by the discontinuity network obtaining in the rock masses behind the slopes.

The orientation of these discontinuities, with respect to the slope face, and their shear strength are major influencing factors on stability. These factors are critical in slopes mined in sedimentary rock formations which are generally weak and stratified. This is the case at Nchanga Open Pit where the hangingwall stands, completely, in generally weak strata of the Upper Roan Dolomites, Shale With Grit, Chingola Dolomite, Dolomitic Schist and Upper Banded Shale. (Fig.16) It is common to see a series of localised bench failures in the Shale With Grit horizon resulting from combined joint, cleavage and blast damage action; ravelling of benches in the Dolomitic Schist and Upper Banded Shale horizons resulting from the same.

LOCATION PLAN
NCHANGA
OPEN
PIT
12E
21000 N
FOOT WALL
ARKOSE/ GRANITE
20800 N
21200 N
1000 M DATUM
DOLSCHIST
C/DOL
HANGING WALL
SWG
URD
SUBS
TFG
BSS
A TYPICAL SECTION
SECTION 12E
SCALE: 1: 2000
Fig.16

Chapter 6

Assessment of the Shear Strength of Rock Discontinuities at Nchanga Open Pit

6.1 Introduction

The bulk of the shear strength information available for use in designing slopes at Nchanga Open Pit (NOP), has been obtained from traditional laboratory strength tests and are interpreted following the Mohr-Coulomb failure criterion. This information has not always proved useful in carrying out rational slope designs, because it is realised that failures in rock slopes cannot be interpreted adequately by the Mohr-Coulomb theory. Stability in rock slopes is not only controlled by the strength of the rock mass as a unit like in soils, but by the shear behaviour of the inherent discontinuities also.

It was, thus, felt appropriate to introduce, in this investigation, a more appropriate method of describing the shear strength of rock formations whose shear behaviour could be attributed to the presence of discontinuities. The shear strength information pertaining to rock types forming the hard overburden of NOP was reviewed following Barton's empirical shear strength criterion. Five rock types were represented in the study, namely:

(i) Shale With Grit (SWG)

(ii) Chingola Dolomite (C/DOL)

(iii) Dolomitic Schist (DOLSCH)

(iv) Upper Banded Shale (UBS) and

(v) The Feldspathic Quartzite (TFQ).

All discontinuities occuring in each of these rocks were classified according to mode of origin, as explained in section 5.4.

Fresh exposures of the above rocks were obtainable between NOP section lines 6E and 9E during the 316-Metre Production Cut. Core samples were available from geotechnical bore-holes drilled in the area.

6.2 Data Acquisition

From the field and laboratory measurements, the index parameters described in the empirical shear strength equation (3) were determined.

6.2.1 Field Measurements

Thirteen different discontinuities were measured in the field. The measurements took the form of:

(i) estimating the joint compressive strength (JCS) using the Schmidt(N-Type) hammer, and

(ii) estimating the joint roughness coefficient (JRC) from visual comparisons between Schmidt comb joint surface impressions and the standard roughness profiles.

A brief description of the rock and the surface characteristics (including the mean JRC and JCS) is given in Table 2. Other details are presented in Appendix A.

6.2.2 Laboratory Measurements

Laboratory work included:

(i) determining the basic angle of internal friction (ϕb) of each rock mass from shear-box tests, and

(ii) estimating the uniaxial compressive strength (UCS) of the rock masses from the results of the point load index tests.

Given in Table 3 is a summary of the results of the point load index test including calculated UCS values of the rocks. Details of the test are given in Appendix B. Figures 17 to 21 are the rectangular plots interpreting shear-box results in terms of mean basic friction angles. To define the residual angle of friction (ϕr) for a

rock discontinuity, Richards (1975) modified empirical relation, equation (6), was used to reduce the experimentally obtained values of the basic friction angles. These are presented in Table 4. Other details of the shear-box test are presented in Appendix C.

6.3 Analysis of Experimental Results

A summary of the parameters obtained from field and laboratory measurements for the purpose of defining the shear strength of a discontinuity is presented in Table 5.

As discussed in section 3.2, Barton (1971a) showed that a straight line curve can be obtained by plotting the strength ratios, τ/σ_n versus JCS/σ_n, on a log-tan scale for each JRC as long as the joint wall compressive strength (JCS) is not exceeded by the effective normal stress (σ_n) acting across such joint.

For each of the five rock types represented in this study, a graphical interpretation of the above principle was undertaken. Figures 22 to 26 were obtained to confirm the validity of the principle in this application. Details of the plotted data, in the joint strength to normal stress ratio range of $1 \leqslant$ JCS/$\sigma_n \leqslant 200$, are given in Table 6.

Table 2 Description of the 13 Discontinuities tested during the investigation

No.	ROCK TYPE	JOINT DISCRIPTION	NO. OF TESTS	DISCONT TYPE	JRC (Mean)	JCS(MPa) (Mean)
1.	SWG	: smooth, planar bedding joints (iron staining)	20	I	8	10
2.	"	: smooth, nearly planar cleavage joints (iron staining)	15	I	4	15
3.	"	: rough, planar blasting fractures (fresh surfaces)	35	II	8	20
4.	C/DOL	: smooth, planar tectonic joints (iron staining)	10	I	8	10
5.	"	: smooth, nearly planar bedding joints (iron staining)	10	I	6	10
6.	"	: rough, planar blasting fractures (fresh surfaces)	20	II	9	20
7.	DOLSCHIST	: rough, planar tectonic joints (slight weathering)	30	I	9	20
8.	"	: rough, non-planar blasting fractures (fresh surfaces)	30	II	10	25
9.	UBS	: smooth, planar bedding joints (weathered)	10	I	4	10
10.	"	: smooth, planar blasting fractures (weathered)	10	II	6	15
11.	TFQ	: rough, planar tectonic joints (malachite staining)	15	I	10	35
12.	"	: rough, planar bedding joints (malachite staining)	15	I	10	35
13.	"	: rough, non-planar blasting fractures (- do -)	15	II	12	55

Table 3 Summary of the Results of the Point Load Index Test

MATERIAL PROPERTIES				P/L INDEX IN DIAMETRAL TEST		
ROCK TYPE	INTACT MAT. STRENGTH CLASSIF'N	CORE SIZE	NO. OF SAMPLES	MEAN Is(50) [MPa.]	MEAN # UCS [MPa.]	% STD. + DEVIATION
SWG	Weak	AQ/BX	30	0.19	4.56	46
	Mod. Strong	"	38	1.44	34.56	31
	Strong	"	22	2.92	70.08	16
	Very Strong	"	20	6.82	163.68	17
C/DOL	Weak	NX/BX	40	0.22	5.28	62
	Mod. Strong	"	32	1.23	29.52	40
	Strong	"	16	3.07	73.68	19
DOLSCH	Weak	NX/BX	14	0.18	4.32	20
	Mod. Strong	"	20	1.28	30.72	25
	Strong	"	26	2.93	70.32	44
	Very Strong	"	38	5.77	138.48	64
UBS	Weak	NX/AXT	36	0.36	8.64	31
	Mod. Strong	"	26	1.14	27.36	47
	Strong	"	12	3.00	72.00	14
	Very Strong	"	14	5.28	126.72	22
TFQ	Mod. Strong	NX/AXT	08	1.62	38.88	24
	Strong	"	20	3.04	72.96	18
	Very Strong	"	20	6.25	150.00	19
	Ext'ly Strong	"	38	12.80	307.20	29

MEAN UCS = 24.Is(50)

+ %STD. DEV is a measure of DISPERSION of the DATA about the MEAN.

$** Core Sizes: AXT = 32mm; BX = 42mm; AQ = 46mm; NX = 54mm.

Fig.17 SHEAR-BOX RESULTS ON FLAT SURFACES OF ROCK TYPE

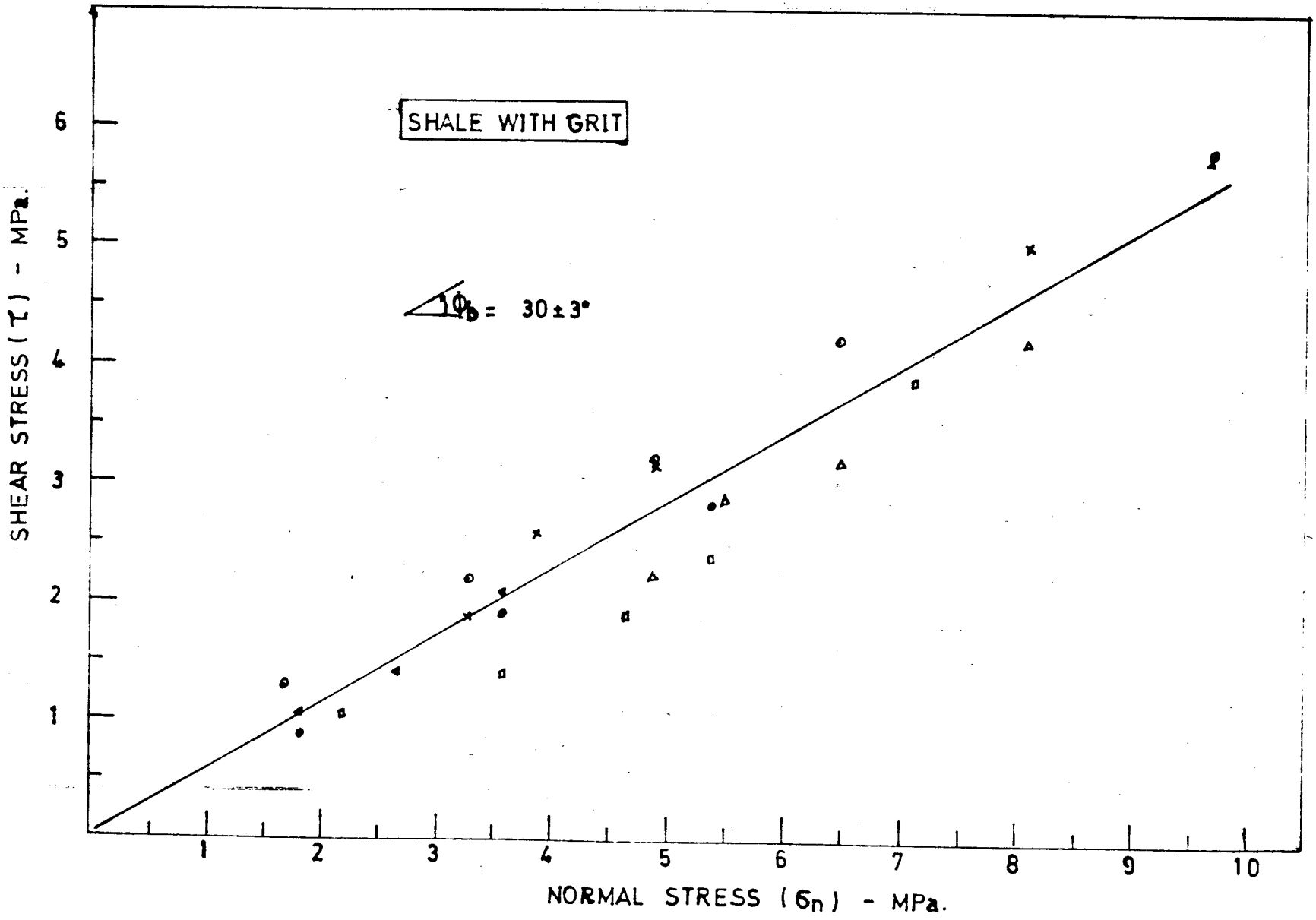

Fig. 18 SHEAR - BOX RESULTS ON FLAT SURFACES OF ROCK TYPE

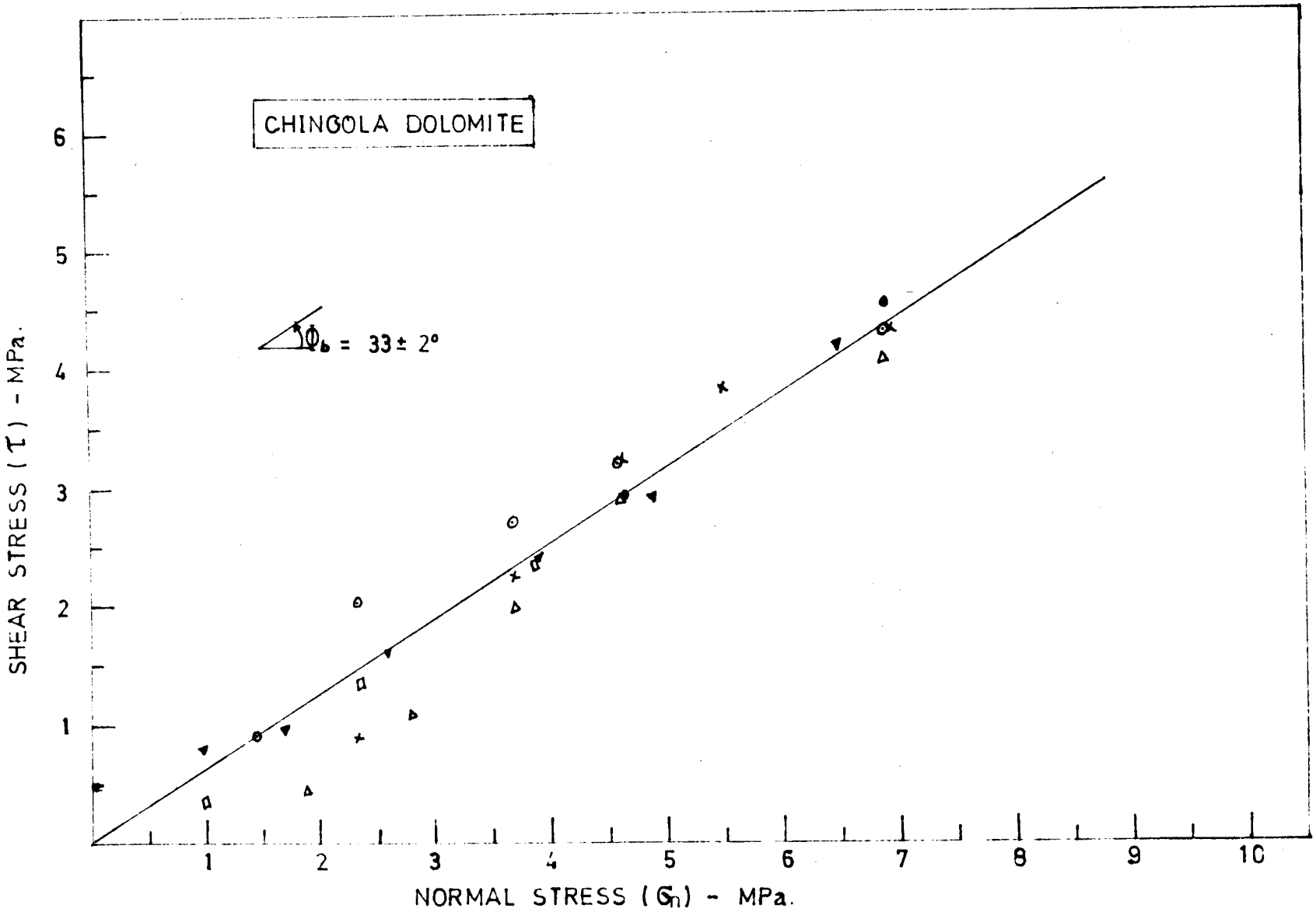

Fig.19 SHEAR-BOX RESULTS ON FLAT SURFACES OF ROCK TYPE

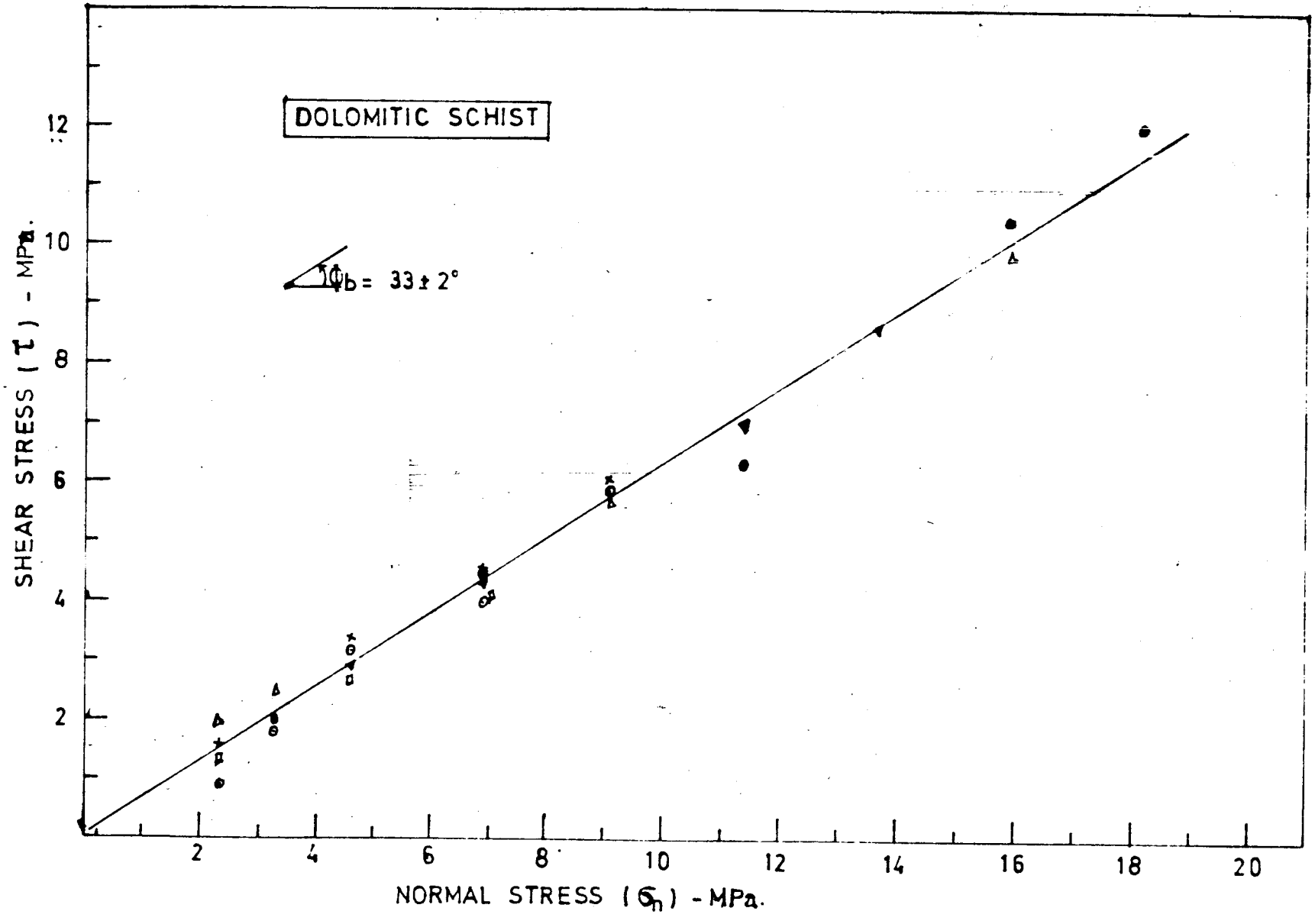

Fig. 20 SHEAR-BOX RESULTS ON FLAT SURFACES OF ROCK TYPE

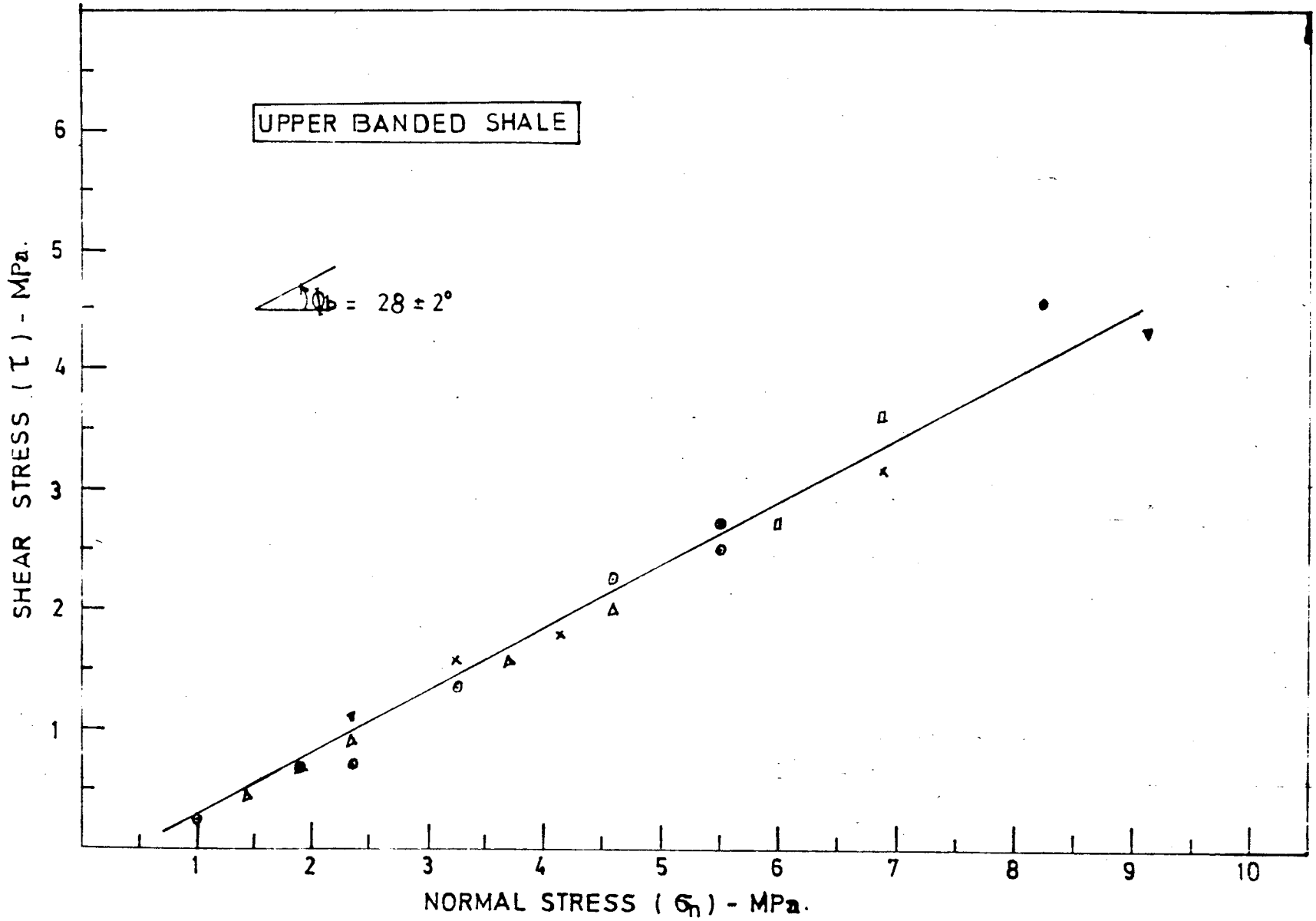

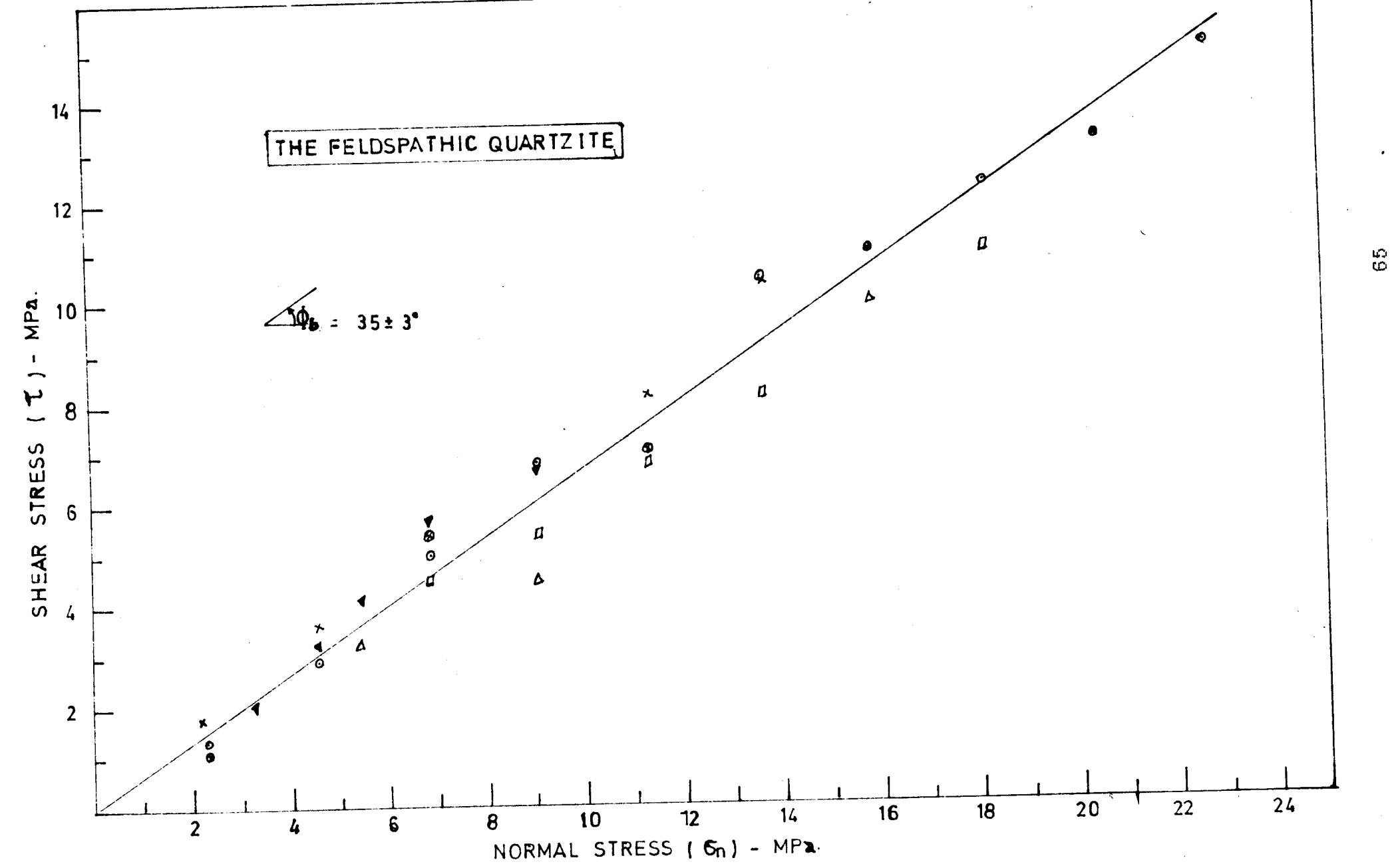
THE FELDSPATHIC QUARTZITE
ϕ_b = 35 ± 3°
SHEAR STRESS (τ) - MPa.
NORMAL STRESS (σ_n) - MPa.
2
4
6
8
10
12
14
16
18
20
22
24

Table 4 A Summary of the calculated Residual Angles of internal friction for the Rocks

ROCK TYPE	* $\phi r = (\phi b - 20) + 20(r/R)$		
	BASIC FRIC'N ANGLE ϕb (Degrees)	SCHMIDT HAMMER REBOUND RATIO (r/R)	RESIDUAL FRIC'N ANGLE ϕr (Degrees)
SWG	30o	0.90	28.0o
C/DOL	33o	0.78	28.5o
DOLSCHIST	33o	0.93	31.6o
UBS	28o	0.90	26.0o
TFQ	35o	0.95	34.0o

* NB: The values for the Residual Angles of internal friction (ϕr) are estimated by Richards (1975) modified empirical equation.

r = Schmidt hammer rebound on weathered joint surfaces
R = Schmidt hammer rebound on dry unweathered rock surfaces.

Table 5 A Summary of the Strength Properties for the Discontinuities

ROCK TYPE	ROCK DENSITY [KN/m3]	MEAN UCS [MPa]	MEAN JCS[MPa]		RESIDUAL FR. ANGLE ϕr [Deg.]	MEAN JRC FOR	
			Type1	Type2		Type1	Type2
SWG	24.5	56.9	15	20	28.0o	6	8
C/DOL	27.5	26.5	10	20	28.5o	7	9
DOLSCHIST	26.5	79.2	20	25	31.6o	9	10
UBS	22.0	41.6	10	15	26.0o	4	6
TFQ	24.0	191.2	35	55	34.0o	10	12

NB: The residual angle of internal friction (ϕr) is common to both discontinuity types.

Table 6 The Empirical Shear Strength Criterion for Rock Discontinuities.

$\tau/\sigma_n = \tan [JRC.\log(JCS/\sigma_n) + \phi_r]$

JCS/σ_n RATIO	SMG ϕ_r = 28.0		C/DOL ϕ_r = 28.5		DOLSCHIST ϕ_r = 31.6		UBS ϕ_r = 26.0		TFD ϕ_r = 34	
	JRC=6	JRC=8	JRC=7	JRC=9	JRC=9	JRC=10	JRC=4	JRC=6	JRC=10	JRC=12
1	0.53	0.53	0.54	0.54	0.62	0.62	0.49	0.49	0.67	0.67
2	0.57	0.59	0.59	0.61	0.68	0.69	0.51	0.53	0.75	0.77
3	0.60	0.62	0.62	0.64	0.72	0.74	0.53	0.55	0.80	0.83
4	0.62	0.64	0.64	0.67	0.75	0.77	0.54	0.57	0.84	0.88
5	0.63	0.66	0.66	0.69	0.78	0.80	0.55	0.58	0.87	0.91
6	0.64	0.68	0.67	0.71	0.80	0.82	0.56	0.59	0.89	0.94
7	0.65	0.69	0.69	0.73	0.82	0.84	0.56	0.60	0.91	0.97
8	0.66	0.71	0.70	0.74	0.83	0.86	0.57	0.61	0.93	0.99
9	0.67	0.72	0.70	0.76	0.84	0.87	0.57	0.62	0.95	1.02
10	0.67	0.73	0.71	0.77	0.86	0.89	0.58	0.62	0.97	1.04
20	0.72	0.79	0.77	0.85	0.94	0.99	0.61	0.67	1.07	1.18
30	0.75	0.83	0.81	0.89	1.00	1.05	0.62	0.70	1.14	1.27
40	0.77	0.86	0.83	0.93	1.04	1.10	0.63	0.72	1.19	1.34
50	0.79	0.89	0.85	0.96	1.07	1.13	0.64	0.73	1.23	1.40
60	0.80	0.91	0.87	0.98	1.10	1.17	0.65	0.74	1.27	1.45
70	0.81	0.92	0.88	1.00	1.12	1.19	0.66	0.76	1.30	1.49
80	0.82	0.94	0.89	1.02	1.14	1.22	0.66	0.77	1.33	1.53
90	0.83	0.95	0.91	1.04	1.16	1.24	0.67	0.77	1.35	1.57
100	0.84	0.97	0.92	1.05	1.17	1.26	0.67	0.78	1.38	1.60
150	0.87	1.01	0.96	1.11	1.24	1.34	0.69	0.81	1.47	1.74
200	0.89	1.05	0.99	1.16	1.29	1.41	0.71	0.83	1.54	1.85

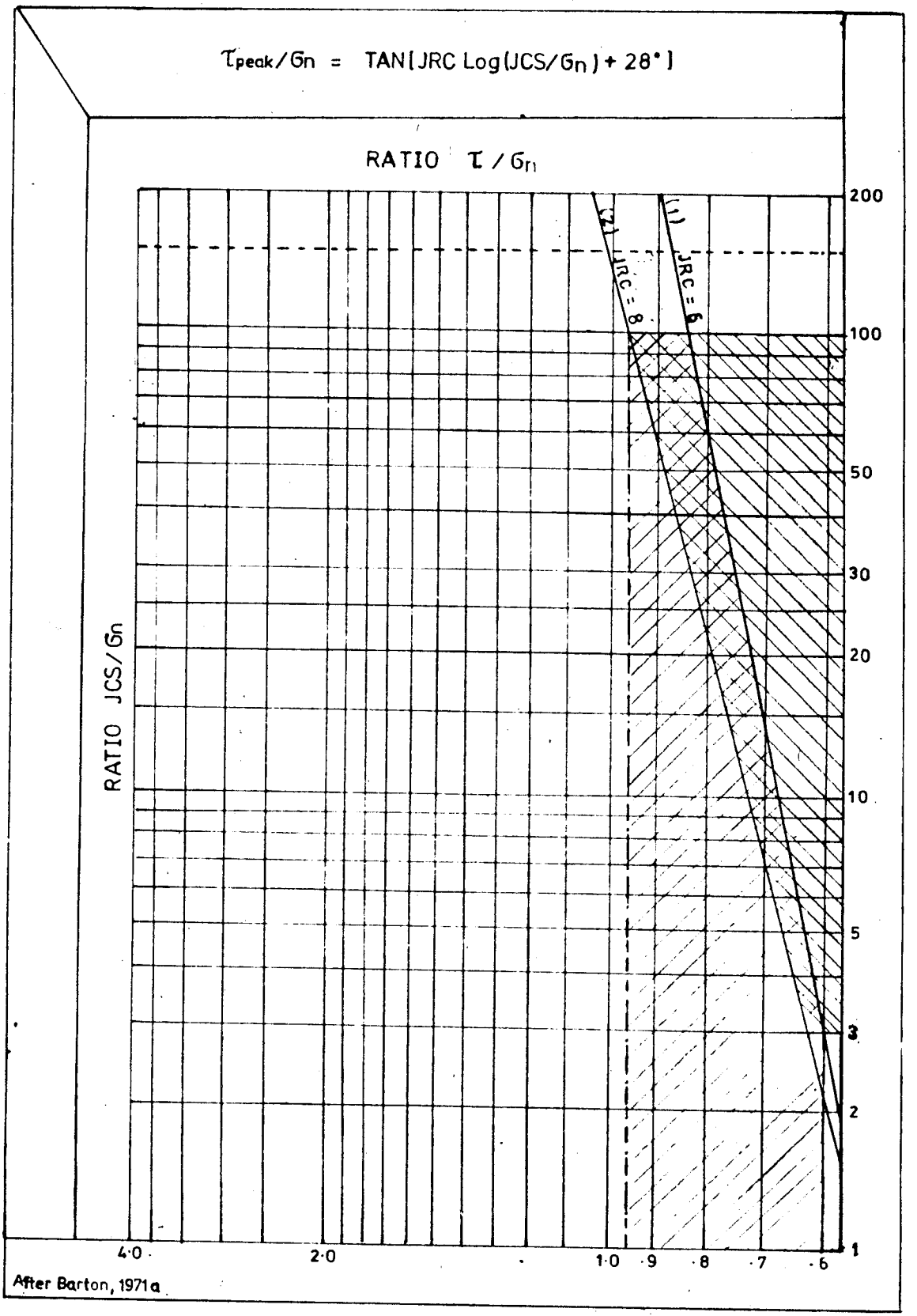

Fig. 22 PEAK SHEAR STRENGTH CRITERION FOR JOINT TYPES 1 & 2 IN THE SHALE WITH GRIT FORMATION.

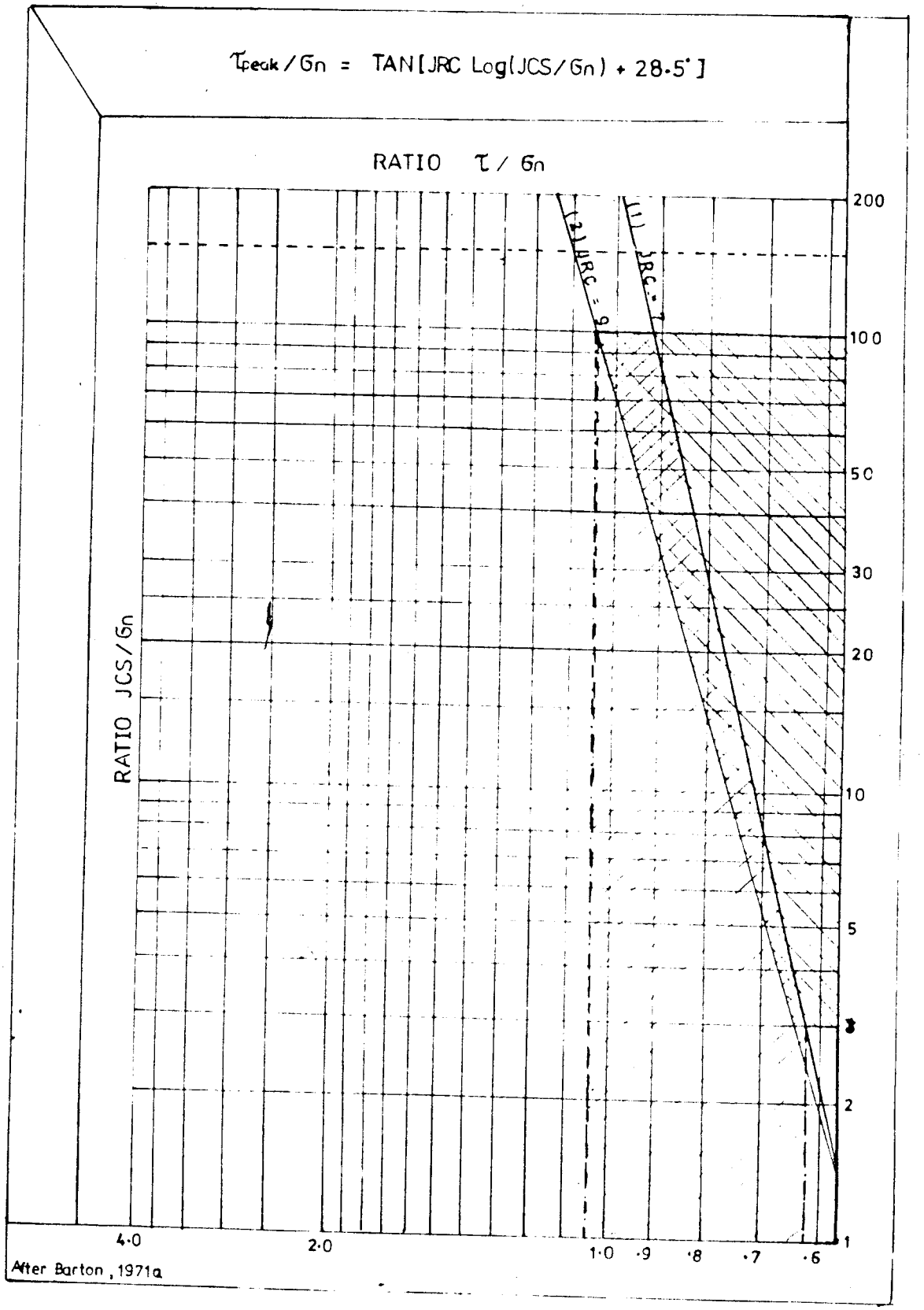

Fig. 23 PEAK SHEAR STRENGTH CRITERION FOR JOINT TYPES 1 & 2 IN THE CHINGOLA DOLOMITE FORMATION.

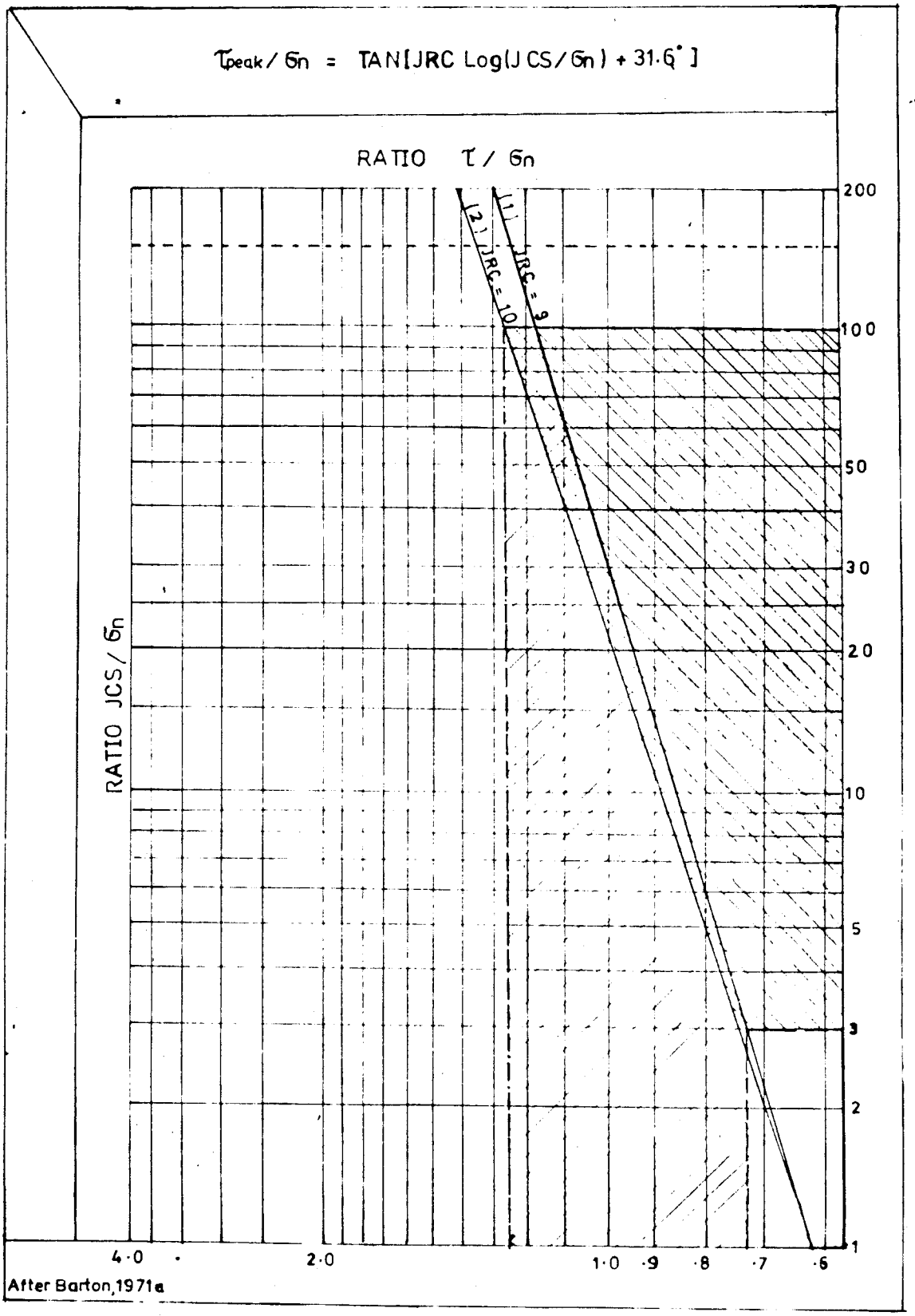

Fig. 24 PEAK SHEAR STRENGTH CRITERION FOR JOINT TYPES 1 & 2 IN THE DOLOMITIC SCHIST FORMATION.

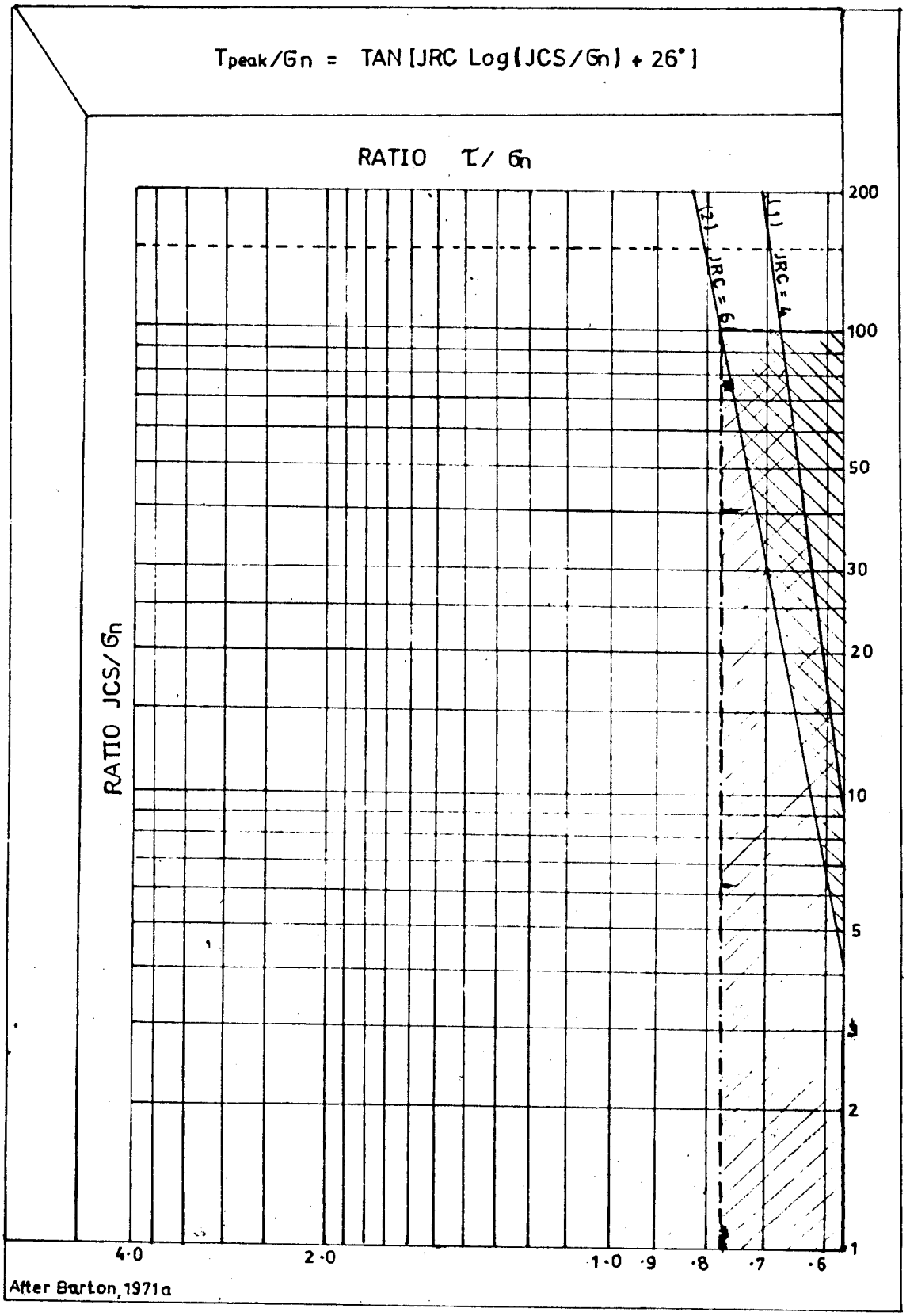

Fig. 25 PEAK SHEAR STRENGTH CRITERION FOR JOINT TYPES 1 & 2 IN THE UPPER BANDED SHALE FORMATION.

6.4 Application of Empirical Shear Strength Values in Slope Stability Calculations

From the foregoing, one is able to deduce that, the choice of shear strength values for use in analysing a rock slope, with respect to stability, depends on a sound understanding of the basic mechanics of failure and the influence of various factors which can alter the shear strength characteristics of a rock mass. For example, the depth at which a failure surface occurs below the crest of the slope, determines the amount of the normal stress acting across it. Depending on the magnitude of the normal stress in relation to the controlling discontinuity wall strength, the measurable peak shear strength value, in terms of total friction angle (arctan $\tau/\sigma n$), is accordingly affected.

The log-tan charts that have been plotted in Figs.22 to 26 are useful in making the choice of the shear strength values. Knowing the anticipated range of normal stress [calculated from equation (7)] and the JCS (easily estimated from Schmidt hammer rebounds), the relevant range of JCS/σn ratio can be calculated. The resulting values can then be read into the corresponding chart from which the respective peak tan($\tau/\sigma n$) values can be read off. Because of

Table 7 Variation of the Peak Shear Strength [arctan(τ/σ_n)] of Rock Discontinuities in the Strength/Stress ratio range: $3 \leq JCS/\sigma_n \leq 100$

ROCK TYPE	RANGE OF PEAK COEFFICIENT OF FRICTION		RANGE OF PEAK ANGLES OF FRICTION [ϕ_p Deg.]	
	Type 1	Type 2	Type 1	Type 2
SWG	0.60 - 0.84	0.62 - 0.97	31.0o-40.0o	31.8o-44.1o
C/DOL	0.62 - 0.92	0.64 - 1.05	31.8o-42.6o	32.6o-46.4o
DOLSCHIST	0.72 - 1.17	0.74 - 1.26	35.8o-49.5o	36.5o-51.6o
UBS	0.53 - 0.67	0.55 - 0.78	27.9o-33.8o	28.8o-38.0o
TFQ	0.80 - 1.38	0.83 - 1.60	38.7o-54.1o	39.7o-58.0o

feature of the program allows the generation of random failure surfaces, in a given slope geometry, making it possible for the user to determine the critical minimum factor of safety more easily. The user simply defines the slope geometry, in rectangular coordinates, and the shear strength parameters 'c' and 'ϕ' for each rock type in the given slope. The user can also define strength anisotropy in each rock type according to the oriantation of the plane of failure across such rock formation. This program is well suited for the application of empirically determined shear strength values in, rationally, analysing the stability of rock slopes.

At Nchanga Open Pit mine, the computer based programs of slope stability analysis have long been incorporated into the main computer frame. Recently the Geotechnical Services - the section responsible for carrying out slope stability calculations - procured an IBM personal computer with additional software for stability anlyses. Latest on the list of STABL software is the **PCSTABL5** program which employs the simplified Bishop, Janbu and Spencer methods of slope stability analyses. Presented in Appendix D are some graphical outputs of the results obtained from the PCSTABL5 version performed on a typical section of the Nchanga Open Pit, with calculations based on the shear strength information presented in this study.

Chapter 7

Conclusion and Recommendations

7.1 Conclusion

The peak shear strength values, in terms of total angles of internal friction (arctan $\tau/\sigma n$) pertaining to rock discontinuities (Type 1 and Type 2) occuring in the Shale With Grit, Chingola Dolomite (competent), Dolomitic Schist, Upper Banded Shale and The Feldspathic Quartzite formations, have been quantified following Barton's empirical shear strength criterion. The results of this work compare very well with the shear strength data compiled from laboratory tests and rock mass classification studies, currently in design use on the Mine (Table 8).

Though this comparison is made here, it is important to note that the shear strength information in design use is applied to the rock as a unit without regard for strength anisotropy and the influence of the effective normal stress distribution behind the slope. These factors have, however, been taken into account in the results of this study. The shear strength values have been assigned to the discontinuity type, and their magnitudes determined by the compressive strength to normal stress ratio. The lower and upper bound shear strength values for each discontinuity type are obtainable at higher and lower levels of the effective normal stress, respectively.

Table 8 Comparison between 'traditiionally' and 'empirically determined friction angle values pertaining to rock type.

ROCK TYPE	RANGE OF TRADITIONAL VALUES ASSOCIATED WITH ROCK TYPE [ϕ Deg.]	RANGE OF EMPIRICAL VALUES* DETERMINED FOR TYPE OF DISCONTINUITY [ϕ Deg.]	
		Type 1	Type 2
SHALE WITH GRIT	30o - 44o	31o - 40o	32o - 44o
C/DOLOMITE " (decomposed)	25o - 30o 15o - 25o	32o - 43o -	33o - 46o -
DOLOMITIC SCHIST	44o - 50o	36o - 50o	37o - 52o
UPPER BANDED SHALE	25o - 37o	28o - 34o	29o - 38o
THE FEL/QUARTZITE	44o - 53o	39o - 54o	40o - 58o

* Values rounded-off to the nearest whole number.

NB: The range of 'traditional' friction angle values is compiled from the results of routine laboratory tests conducted at the Mine.

One other advantage of using empirical shear strength data is in avoiding over-designed slopes. The advantage here is that the shear strength information is quantified in relation to the stability governing strength/stress ratio, JCS/σ_n, and it is defined by a straight line relationship on a log-tan chart as shown in Figs.22 to 26. A relevant choice of arctan(τ/σ_n) values for use in design is made easier. If plotted for each rock type in each structural zone the log-tan charts could provide a good basis for shear strength prediction and extrapolation.

7.2 Recommendations

In the stability analysis of any rock slope, the principles around which such analysis must evolve are a study of:

(i) the system of jointing, which involves a careful assessment of their trends and genetic relationships with the geological environment;

(ii) the strength parameters of the discontinuities, which includes an investigation of the properties of both the planes of weakness and any infilling material occuring between them;

Arising from the interpretation of the shear strength results presented in this study, there is good reason to believe that the peak shear strength of the discontinuities occuring in the hangingwall rock masses of the Nchanga Open Pit will reduce to residual strength for much smaller displacements before slope failure, owing to their low roughness coefficients (JRC range 4 - 12) and wall compressive strengths (JCS range of 10 - 25 MPa). This should be born in mind when designing final slopes of the open pit. There is, also, need to recommend berm preservation to minimise unwanted damage to existing or remaining slopes. Full scale application of controlled blasting techniques at Nchanga Open Pit have been thwarted by the non-availability of suitable drilling equipment. However, the importance of controlled blasting in huge open cast mining operations cannot be over-emphasized.

oooooooooooooooooo

BIBLIOGRAPHY

Barton N.R. (1971a) Relationship between Joint Roughness and Joint Shear Strength. Proc. Int. Symp. Rock Mech. Nancy, Rock Fracture Paper 1, 8.

Barton N.R. (1972) A Model Study of Rock Joint Deformation. IJRM Sci. and Geomech. Abstr. Vol. 9, pp 579 - 607.

Barton N.R. (1973) Review of a New Shear Strength Criterion for Rock Joints. Engineering Geology 7, pp 287 - 332.

Barton N.R. (1976) The Shear Strength of Rock and Rock Joints. IJRM Sci. and Geomech. Abstr. Vol. 13 No.9.

Barton N.R. and Choubey V. (1977) The Shear Strength of Rock Joints in Theory and Practice. Rock Mechanics 10, pp 1 - 54.

Barton N.R. ; Bandis S. and Lumsden A.C. (1981) Experimental Studies of Scale Effects on the Shear Behaviour of Rock Joints. IJRM Sci. and Geomech. Abstr. Vol.18 No.1, pp 1 - 20.

Bauer A. and Calder P.N. (1970) The Influence and Evaluation of Blasting on Stability. Proc. 1st Int. Conf. on Stability in Open Pit Mining, Vancouver B.C. Canada (Nov.23 - 25), pp 23 - 45.

Bieniawski Z.T. (1974) Estimating the Strength of Rock Materials. Journal of the South African Institute of Mining and Metallurgy Vol. 74, pp 312 - 320.

Bieniawski Z.T. (1975) The Point Load Test in Geotechnical Practice. Engineering Geology Vol. 9, pp 1 - 11.

Brach E. and Franklin J.A. (1972) The Point Load Index Strength Test. IJRM Sci. and Geomech. Abstr. Vol. 9, pp 669 - 697.

Brook N. (1977) A Method of Overcoming both Shape and Size Effects in Point Load Testing. Proceedings of a Conference on Rock Engineering, U.K. New Castle Upon Tyne (April), pp 53 - 70.

Brook N. (1980) Size Correction for Point Load Testing Technical Note: IJRM Sci. and Geomech. Abstr. Vol. 17, pp 23 - 235.

Brook N. (1985) The Equivalent Core Diameter Method of Size and Shape Correction in Point Load Testing. IJRM Sci. and Geomech. Abstr. Vol. 22, pp 61 - 70.

Brown E.T. (1981) Rock Characterisation, Testing and Monitoring. ISRM Suggested Methods.

Budavari S. (Ed.) Rock Mechanics in Mining Practice. Monograph Series No.5 of the South African Institute of Mining and Metallurgy.

Calder P.N. and Morash B.J. (1970) "Pit Wall Control at Adams Mine." Paper presented at American Mining Congress of Metal Mining and Industrial Minerals Convention. Denver, Colorado (September).

Carter P.G. and Sneddon M. (1977) Comparison of Schmidt Hammer, Point Load and Unconfined Compression Tests in Carboniferous Strata. Proceedings of a Conference on Rock Engineering, U.K., New Castle Upon Tyne (April), pp 197 - 210.

Dalgleish I.R. (1978) A Geotechnical Case Study of the Hanging Wall Rocks of Nchanga Open Pit. MSc. Thesis, University of Durham.

Diederix D. (1977) The Geology of the Nchanga Mining Licence Area. NCCM Ltd. Chingola Division Internal Report (September).

Duvall W.I. and Fogelson D.W. (1962) Review of Criteria for Estimating Damage to Residences from Blasting Vibrations. USBM Report of Investigations No.5968.

Edwards A.T. and Northwood T.D. Experimental Studies of the Effects of Blasting on Structures. The Engineer, September 1960.

Fecker E. and Rengers N. (1971) Measurement of large scale Roughnesses of Rock Planes by means of Profilograph and Geological Compass. Proc. Int. Symp. Rock Mech. Nancy, Rock Fracture Paper 1, 18.

Goodman R.E. (1970) The Deformability of Joints. American Society for Testing and Materials, STP 477, pp 174 - 196.

Hoek E. (1970) Estimating the Stability of Excavated Slopes in Open Cast Mines. Transactions/Section A, Mining Industry Vol. 79 (October),pp A 109 - 132.

Hoek E. and Bray J.W. (1981) Rock Slope Engineering. Revised Third Edition, IMM.

Hudson J.A. and Priest S.D. (1979) Discontinuities and Rock Mass Geometry. IJRM Sci. and Geomech. Abstract Vol. 16, pp 339 - 362.

Piteau D.R. (1970) Genesis and Characterization of Jointing in the Nchanga Open Pit for Purposes of Ultimately Assessing the Slope Stability. NCCM - Chingola Division, (December) Internal Report.

Rengers N. (1970) Influence of the Surface Roughness on the Friction Properties of Rock Planes. Proc. 2nd Congress of Int. Soc. for Rock Mechanics, Belgrade Vol. 1, pp 229 - 234.

Richards L.R. (1975) The Shear Strength of Joints in Weathered Rock. Ph.D. Thesis. University of London, Imperial College.

Schneider H.J. (1976) The Friction And Deformation Behaviour of Rock Joints. Rock Mechanics (Springer-Verlag) 8, pp 169 - 184.

Siegel R.A. (May,1975b), "STABL Users Manual". Joint Highway Research Project No. 75-9, School of Civil Engineering. Purdue University, West Lafayette, Indiana [Revised by E. Boutrup, June 1978].

Steffen, Robertson and Kirsten (SRK) Report No. 1042/18 (April 1981). Proposed Exploratory Investigations for Final Open Pit Slope Design.

SRK Inc. Report No. 1042/19 (July 1981). Evaluation of Material Properties: Nchanga Open Pit Mine.

SRK Inc. Report No. MI 1042/22 (April 1984). Rock Mass Classifications for Slope Studies at Nchanga Open Pit.

APPENDICES

APPENDIX A

SCHMIDT HAMMER AND SCHMIDT COMB FIELD MEASUREMENTS

A.1 Determination of the Joint Wall Compressive Strength (JCS) by Schmidt hammer Method.

A Schmidt hammer [N-Type] is an instrument developed in Germany to measure the compressive strength of concrete cubes. Its application has also been extended to rock mechanics in estimating the compressive strength of rock samples. Its principle of operation is simply a steel ball inside it which, after the release of a catch, travels a fixed distance under spring pressure. The ball is designed to develop a kinetic energy of 0.225 mKg on striking an anvil held against the rock under test. The anvil has a flattened nose-piece to produce the blow. The instrument may be pointed at the rock in any direction normal to the rock surface, but the gravitational effect on rebound values, due to the inclination of the tool must be accounted for.

To make it easy for the user, the instrument is usually supplied with a correlation chart (Fig. A-1) which is used to interpret the rock strength in relation to rebound numbers. Correlation curves are drawn for general angles of inclination of the instrument in a

testing position. These are, +90 & +45 degrees for instrument held facing upwards; 0o for instrument held in a horizontal position and -90o & -45o for instrument held facing downwards. Rebound numbers obtained at any other angles can be treated by interpolation between successive curves.

A.1.1 Test Procedure

i) Select suitable surfaces of the discontinuities occuring in the rock mass in-situ. Clean-off surface, if possible, to remove any foreign material or dust.

ii) Hold Schmidt hammer normal to the surface of the discontinuity and press pointed end (anvil) of hammer against the surface to release the catch. Take note of the angle of inclination of the tool to account for the effect of gravity on the steel ball. Obtain several rebound numbers from each surface. Calculate the average rebound number for the surface from at least five readings ranking high on the scale.

iii) Read the mean rebound numbers, calculated in (ii), into the correlation chart accompanying the Schmidt hammer and obtain

the corresponding compressive strength. The value of the compressive strength obtained represents the Joint Wall Compressive Strength (JCS).

A.2 Estimation of the Joint Roughness Coefficient (JRC) by Schmidt Comb Method.

A Schmidt comb is a simple instrument made in form of a double edged comb. It is infact a wire comb. Thin steel wires (about 0.5mm dia.) are closely packed in a slotted metal frame measuring about 15cm long. Wires are only free to move in the axial direction (up and down the slot) when pressed against the surface. To obtain an impression of the surface profile, the individual wires should be made to touch the surface. This can be achieved by pressing each wire with a finger from the free edge until it touches the surface being measured. When this is done, the free edge of the comb will take up the shape of the surface profile which can be traced on paper for visual comparison with standard roughness profiles.

A.2.1 Test Procedure

i) Clean-off the discontinuity surfaces to be measured.

ii) Press Schmidt comb firmly against the surface. Obtain several impressions along the direction of greatest dip and trace them on paper.

iii) Compare the impressions obtained with the standard roughness profiles recommended by ISRM. Obtain the range of roughness coefficients associated with the profiles matching the impressions. Calculate the average of at least five prominent impressions. The average value obtained represents the Joint wall Roughness Coefficient (JRC) - see Table A-1.

oooooooooooooooooo

Fig. A-1 **Cube Compressive Strength in kg/cm² plotted against the Rebound Number**

Type N Test Hammer

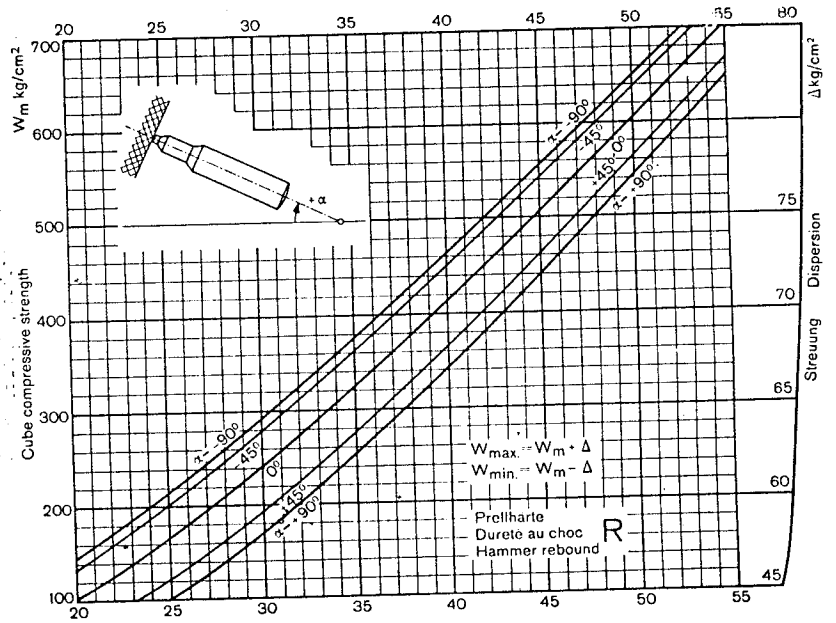

The curves apply to compact Portland cement concrete with good quality gravel/sand aggregate. Age 14 to 56 days. Smooth and dry concrete surface.

W_m = most likely value of the cube compressive strength in kg/cm².

The dispersion limits $W_{max.}$ and $W_{min.}$ are so defined that they include 80 percent of all the test results.

Note under Section IV "Limits of Validity of the Calibration Curves"!

TABLE A-1

ROCK MASS DISCRIPTION SHEET.

NCHANGAO / PIT HANGINGWALL.

A Summary Sheet.

ROCK TYPE	INTACT MAT. STRENGTH	S/HAMMER REBOUNDS	JCS RANGE [MPa]	JOINT DISCRIPTION	SCHMIDT COMB PROFILE AND JRC.	COMMENTS
S W G	Strong	*I. 26	20	Bedding & cleavage	: 6	Staining visible on bedding/cleavage planes; fracture planes fresh.
		II. 30	25	Blasting fractures	: 8	
C/DOL	Mod. Strong	I. 18/22	10 - 15	Bedding & joints	:10	Rock mass intact; staining on all joint planes; fracture surfaces fresh.
		II. 17/21	10 - 15	Fracture surfaces	:10	
DOLSCHIST	Very Strong	I. 25/32	20 - 30	Shear joints	: 4	Rock material intact but slightly weathered; staining on all joint surfaces.
		II. 23/31	20 - 30	Fracture surfaces	:12	
U B S	Weak	I. 12	< 10	Bedding & joints	: 4	Rock mass highly weathered; staining on all joint surfaces.
		II. 12	< 10	Fracture surfaces	: 8	
T F Q	Very Strong	I. 26/35	20 - 35	Bedding & joints	:10	Rock material slightly weathered; copper sulphate staining into the rock material.
		II. 31/35	30 - 35	Blasting fractures	:14	

* I & II Refer to discontinuity types 1 & 2 in the investigation.

APPENDIX B

POINT LOAD INDEX STRENGTH TESTING: STANDARD PRACTICE

B.1 Determination of the Rock Strength Index (Is)

The Point Load Index testing machine is a cheap and easy to handle equipment designed for rock strength index testing. The test is simple and inexpensive. It can be carried out on unprepared rock core samples also.

There are two types of point load machines available commercially:

(i) the Point Load Index test equipment manufactured by Robertson Research Ltd., Llandudno, North Wales; and

(ii) the Point Load test equipment manufactured by Engineering Laboratory Equipment Ltd., Hemel Hempstead, Hertfordshire, England.

The first type was used in this investigation.

B.1.1 Test Procedure

(a) Select specimens of suitable dimensions.

ii. UNDER NO CIRCUMSTANCES MAY THE SPECIMEN BE LOADED BEYOND THE LIMITS OF THE GAUGE FITTED. This would result in severe damage of the pressure gauge unit. If the strength is more than 50 KN, it should be noted as such.

(g) Reject the test as invalid if the fracture produced passes through only one loading point [see Fig.B-1(b)].

(h) Record the failure load 'P' to the nearest 1.0 KN.

NOTES

(i) **Moisture Content** - Most specimens are tested at 'core-shed' (cs) moisture content, which varies between rock types and over different periods of storage.

(ii) **Strength Anisotropy** - In shaley/schistose rocks, specimens should be tested in directions which will give both the highest and least strength values; i.e. normal and parallel to planes of weakness. Strength Anisotropy Index, Ia(50), is the ratio of the mean Is(50) values measured normal and parallel to weakness planes [Fig.B-1(c)].

(iii)**Gauge Sensitivity** - Depending on the intact material strength of the specimen, the choice can be made from the range of pressure gauges accompanying the instrument. For example, the Robertson Research Point Load Machine is accompanied by the 3KN, 5KN, 11KN, 25KN and 50KN pressure gauges, arranged in the order of reducing sensitivity.

B.1.2 Calculation of the Strength Index Is(50).

The 'uncorrected' strength index (Is) is calculated from an equation:

$$Is = P/De^2$$

where P = load at failure

De = distance between platens

De = D for diametral tests

De = 12.57A for axial, block and lump tests

A = minimum x-section area of failure through platen contact points [Fig.B-1(a)].

However, before calculation of the standard point load strength index Is(50), the values for 'De' are adjusted to a standard size of 50mm core diameter. This is done using the size correction chart (Fig.B-2) or by the application of the size correction factor,'F'. The size correction factor (F) is calculated following the sequence below:

(i) Determine De, depending on the type of test (i.e diametral, axial etc.);

(ii) Calculate size correction factor, F:

$$F = (De/50)^{0.45}$$

(iii) Calculate corrected point load strength index, $Is(50) = F(P/De^2)$ in units of MPa.

(iv) Mean Is(50) values are calculated by ignoring the two highest and the two lowest values on the data sheet, and finding the arithmetic mean of the remainder.

Tables B1 and B2 are samples of a typical point load data sheet.

oooooooooooooooooo

APPENDIX B

POINT LOAD TESTING: DIAGRAMS FOR ILLUSTRATION.

(a) SPECIMEN SHAPE REQUIREMENTS

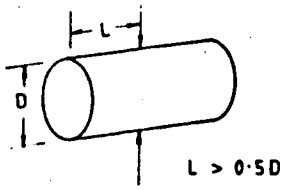

Diametral Test

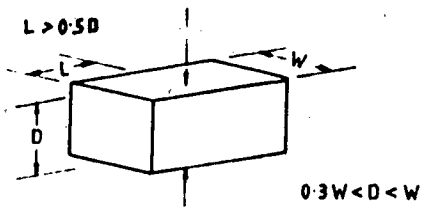

Block Test

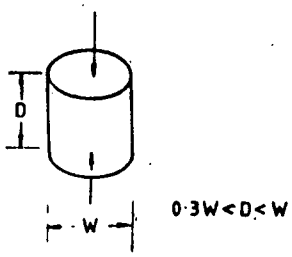

Axial Test

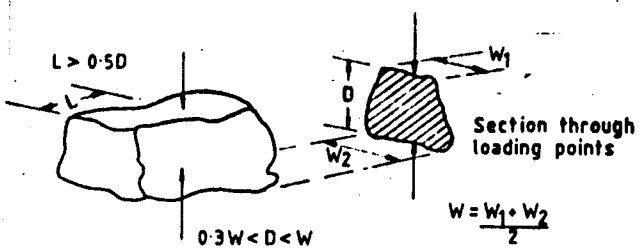

Irregular Lump Test

(b) MODES OF FAILURE AND INVALID TESTS

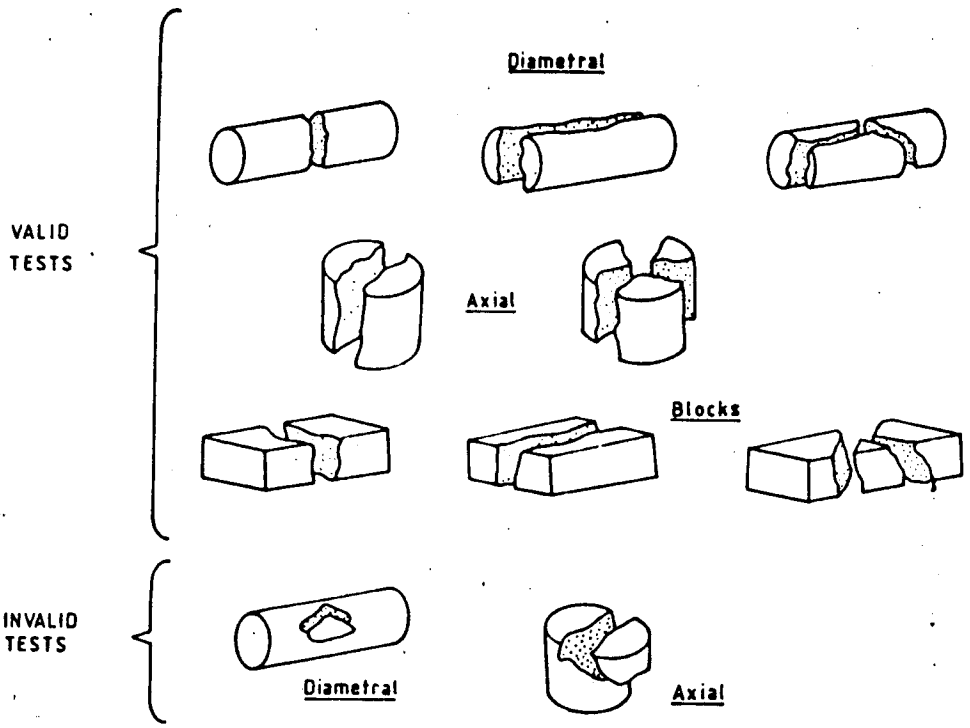

(c) LOADING DIRECTIONS FOR TESTS ON ANISOTROPIC ROCK

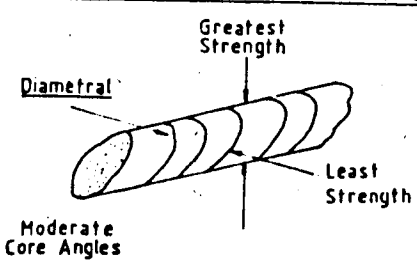

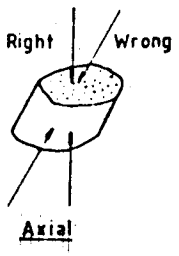

$$I_{a(50)} = \frac{I_{s(50)}\ \text{Greatest}}{I_{s(50)}\ \text{Least}}$$

(See reference ISRM, 1985)

IDEAL DIRECTIONS

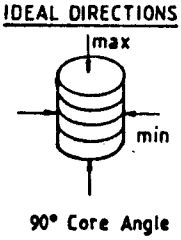

FIG. B-1

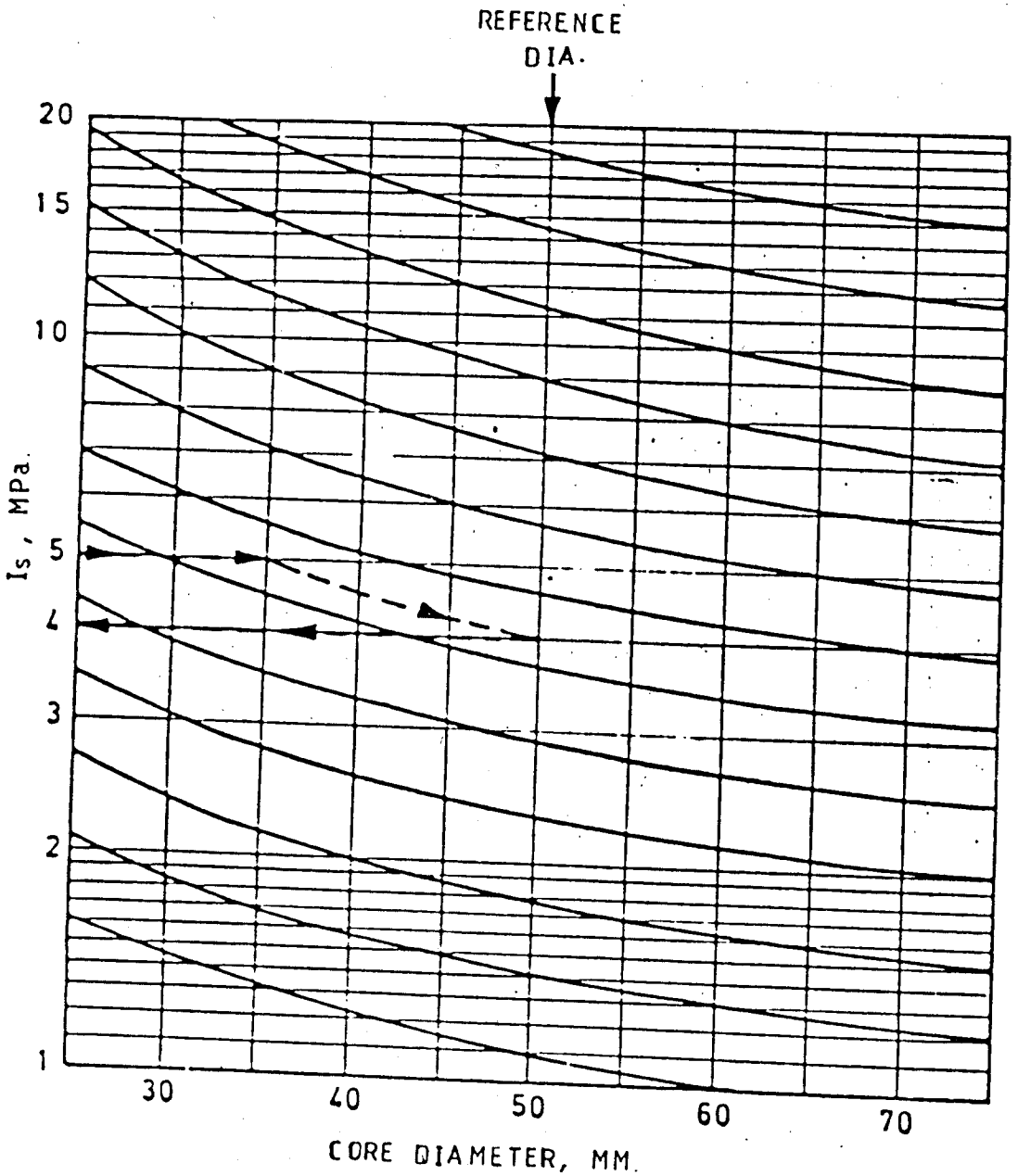

Fig. B-2 SIZE CORRELATION CHART (After Broch & Franklin 1972)

TABLE B.1

POINT LOAD DATA SHEET

B/H NO. NOP 208 LOCATION NOP SECT 4 E. COLLAR ELE. 1278.0M

TESTED BY F.M. DATE 26/08/86

NO./ DEPTH [M]	ROCK TYPE	TEST TYPE			CORE MC		DIST. D [mm]	LOAD [Kn]	FAILURE		STR. INDEX Is(50) [MPa]
		D	A	I	CS	W			IR	APW	
1	SWG	x			x		46	1.20		x	0.55
2	"	x			x		"	1.20		x	0.55
3	"	x			x		"	0.20		x	0.09
4	"	x			x		"	0.90		x	0.41
5	"	x			x		"	2.80	x		1.27
6	"	x			x		"	3.80	x		1.73
7	"	x			x		"	0.10		x	0.05
8	"	x			x		"	0.10		x	0.05
9	"	x			x		"	3.00		x	1.37
10	"	x			x		"	7.00	x		3.19
11	"	x			x		"	3.40	x		1.55
12	"	x			x		"	7.50	x		3.41
13	"	x			x		"	14.00	x		6.38
14	"	x			x		"	10.50	x		4.78
15	"	x			x		"	17.50	x		7.97
16	"	x			x		"	6.40	x		2.91
17	"	x			x		"	18.00	x		8.20
18	"	x			x		"	3.40	x		1.55
19	"	x			x		"	18.50	x		8.42
20	"	x			x		"	5.80	x		2.64
21	"	x			x		"	2.10	x		0.96
22	"	x			x		"	18.00	x		8.20

APPENDIX B

TABLE B.2

POINT LOAD DATA SHEET

B/H NO. LAB CORE LOCATION NOP SECT 6-8 E. COLLAR ELE. 1110.0M

TESTED BY F.M. DATE 27/08/86

NO./ DEPTH [M]	ROCK TYPE	TEST TYPE			CORE MC		DIST. D [mm]	LOAD [Kn]	FAILURE		STR. INDEX Is(50) [MPa]
		D	A	I	CS	W			IR	APW	
1	C/DOL	x			x		54	9.80	x		3.48
2	"	x			x		"	9.30	x		3.30
3	"	x			x		"	11.80	x		4.19
4	"	x			x		"	1.80	x		0.64
5	"	x			x		"	1.60	x		0.57
6	"	x			x		"	4.00	x		1.42
7	"	x			x		"	8.00	x		2.84
8	"	x			x		"	4.00	x		1.42
9	"	x			x		"	6.40	x		2.27
10	"	x			x		"	2.00	x		0.71
11	"	x			x		"	1.00		x	0.36
12	"	x			x		"	1.90	x		0.67
13	"	x			x		"	1.00		x	0.36
14	"	x			x		"	1.30	x		0.46
15	"	x			x		"	5.60	x		1.99
16	"	x			x		"	4.30	x		1.53
17	"	x			x		"	5.30	x		1.88
18	"	x			x		"	7.20	x		2.56
19	"	x			x		"	8.60	x		3.05
20	"	x			x		"	4.60	x		1.63
21	"	x			x		"	2.40	x		0.85
22	"	x			x		"	5.50	x		1.95

APPENDIX C

SHEAR-BOX TEST FOR BASIC FRICTION ANGLE OF ROCK

C.1 Determination of the Basic Friction Angle of Rock.

The Shear-Box test equipment is available in several types commercially. Some of the types have been given in Chapter 3. The types range from simple and cheap portable units to large scale , electrically powered expensive units.

The main purpose of the shear-box test, is to determine the shear strength of the rock in terms of cohesion 'c' and angle of internal friction 'ϕ'.

C.1.1 Specimen Preparation

(a) Obtain intact core samples of NX or larger size.

(b) Select core of reasonable length, of say 7cm or more, which when cut in half can provide specimens that can be conveniently handled in the shear-box moulds.

(c) Use a diamond power saw to cut the samples in halves carefully.

(d) Use the core grinder to obtain a flat and smooth finish of the cut surfaces.

(e) Prepare plaster or concrete mortar and place it in the shear-box moulds.

(f) Pair up the prepared test specimens and cast them in the mortar placed in the moulds, leaving a free end of about 1.0cm. Allow time for the castings to set before stripping the moulds.

(g) Leave the castings to cure fore some time (say 7 days in the case of concrete mortar) before testing. This is important if the cast has to assume high strength to withstand the normal loads in the shear-box at test.

C.1.2 Testing Procedure

(a) Place each pair of the casted and cured specimens into the shear-box unit.

(b) Before applying normal load onto the top half of the box, ensure that core ends are in flash contact.

(c) Apply the initial normal load and record it. Apply the shear load steadly in order to be able to detect the load at which the top half begins to shear along the contact in relation to the bottom half.

(d) Record the shear load. Release the normal load and reposition the top half. Increase

or decrease the normal load, as the case may be, and repeat the test. Continue until contact surfaces of core are impaired. See Tables C-1 to C-5.

(e) Calculate specimen area of contact (usually taken as the gross x-section area) and convert the normal and shear loads to stresses (i.e. load divided by area). Note that, it is only possible to increase the normal stress to a value lower than the specimen's uniaxial compressive strength.

(f) Test several paired samples of the same rock type and plot the corresponding normal versus shear stresses on square charts.

(g) Fit a straight line curve to the plotted points and measure the slope of the curve. The slope of the curve is a measure of the basic angle of internal friction [$\phi b = \arctan(\tau/\sigma n)$].

NB. Test results obtained from the same rock type can be plotted on one chart so that the mean value of the friction angle is obtained from a carefully fitted straight line curve.

oooooooooooooooooo

APPENDIX C

Table C-1 SHEAR-BOX TEST DATA SHEET

ROCK TYPE: Shale With Grit LOCATION: N.O.P SECTION: 8 E

TESTED BY: ---------- DATE: ----------

SAMPLE No. 1	c.s.a = 0.00312 m²					No. 2	c.s.a = 0.00312 m²			
N/LOAD (KN)	5.2	10.2	15.2	20.2	30.2	10.2	12.2	15.2	20.2	25.2
S/LOAD (KN)	4.0	7.0	10.0	13.0	18.0	6.0	8.0	10.5	13.0	15.5

No. 3	c.s.a = 0.00312 m²					No. 4	c.s.a = 0.00283 m²			
N/LOAD (KN)	15.2	17.2	20.2	25.2	30.2	6.2	10.2	13.2	15.2	20.2
S/LOAD (KN)	7.0	9.0	10.0	13.0	18.0	3.0	4.0	5.5	7.0	11.0

No. 5	c.s.a = 0.00283 m²					No. 6	c.s.a = 0.00283 m²			
N/LOAD (KN)	15.2	10.2	7.7	5.2	2.2	15.2	10.2	5.2	-	- -
S/LOAD (KN)	8.0	6.0	4.0	3.0	-	8.0	5.5	2.5	-	- -

Table C-2 SHEAR-BOX TEST DATA SHEET

ROCK TYPE: Chingola Dolomite LOCATION: N.O.P SECTION: 7-8 E.

TESTED BY: ---------- DATE: ----------.

SAMPLE No. 1	c.s.a = 0.00221 m²					No. 2	c.s.a = 0.00221 m²			
N/LOAD (KN)	3.2	5.2	8.2	10.2	15.2	5.2	8.2	10.2	12.2	15.2
S/LOAD (KN)	2.0	4.5	6.0	7.0	9.5	2.0	5.0	7.0	8.5	9.5

No. 3	c.s.a = 0.00221 m²					No. 4	c.s.a = 0.00221 m²			
N/LOAD (KN)	4.2	6.2	8.2	10.2	15.2	2.2	5.2	-	-	-
S/LOAD (KN)	1.0	2.5	4.5	6.5	9.0	0.8	2.4	-	-	-

No. 5	c.s.a = 0.00221 m²					No. 6	c.s.a = 0.00312 m²			
N/LOAD (KN)	15.2	10.2	7.2	5.2	3.2	3.2	5.2	8.2	15.2	20.2
S/LOAD (KN)	10.0	6.5	-	3.0	-	2.5	3.0	5.0	9.0	13.0

Table C-3 SHEAR-BOX TEST DATA SHEET

ROCK TYPE: Dolomitic Schist LOCATION: N.O.P SECTION: 7 - 10 E.

TESTED BY: ---------- DATE: ----------

SAMPLE No. 1	c.s.a = 0.00221 m²					No. 2	c.s.a = 0.00221 m²			
N/LOAD (KN)	5.2	7.2	10.2	15.2	20.2	5.2	10.2	15.2	20.2	-
S/LOAD (KN)	3.0	4.0	7.0	9.0	13.0	3.5	7.5	10.0	13.5	-

No. 3	c.s.a = 0.00221 m²					No. 4	c.s.a = 0.00221 m²			
N/LOAD (KN)	5.2	7.2	10.2	15.2	20.2	5.2	7.2	10.2	15.2	20.2
S/LOAD (KN)	3.0	4.5	6.0	9.0	13.0	4.5	5.5	7.0	-	12.5

No. 5	c.s.a = 0.00221 m²					No. 6	c.s.a = 0.00221 m²			
N/LOAD (KN)	30.2	25.2	20.2	15.2	10.2	5.2	15.2	25.2	35.2	40.2
S/LOAD (KN)	19.0	15.0	13.0	9.5	6.5	3.0	10.0	14.0	23.0	26.5

Table C-4 SHEAR-BOX TEST DATA SHEET

ROCK TYPE: Upper Banded Shale LOCATION: N.O.P SECTION: 7 E.

TESTED BY: ---------- DATE: ----------.

SAMPLE No. 1	c.s.a = 0.00221 m²					No. 2	c.s.a = 0.00221 m²			
N/LOAD (KN)	2.2	5.2	7.2	10.2	12.2	5.2	7.2	9.2	12.2	15.2
S/LOAD (KN)	0.5	2.0	3.5	4.5	5.5	2.0	3.5	4.0	6.0	7.0

No. 3	c.s.a = 0.00221 m²					No. 4	c.s.a = 0.00221 m²			
N/LOAD (KN)	3.2	5.2	8.2	10.2	12.2	15.2	13.2	10.2	7.2	5.2
S/LOAD (KN)	1.0	2.0	3.5	4.5	5.5	8.0	6.0	4.5	3.0	2.0

No. 5	c.s.a = 0.00221 m²					No. 6	c.s.a = 0.00221 m²			
N/LOAD (KN)	5.2	-	-	-	20.2	4.2	8.2	12.2	15.2	18.2
S/LOAD (KN)	2.5	-	-	-	9.5	1.5	3.5	6.0	8.0	10.0

Table C-5 SHEAR-BOX TEST DATA SHEET

ROCK TYPE: The Feldspathic Quartzite LOCATION: N.O.P SECTION: 7 E.

TESTED BY: ---------- DATE: ----------.

SAMPLE No. 1	c.s.a = 0.00221 m^2					No. 2	c.s.a = 0.00221 m^2			
N/LOAD (KN)	10.2	15.2	20.2	40.2	50.2	10.2	15.2	20.2	25.2	30.2
S/LOAD (KN)	6.5	11.0	15.0	27.0	33.0	8.0	12.0	15.0	18.0	23.0

No. 3	c.s.a = 0.00221 m^2					No. 4	c.s.a = 0.00221 m^2			
N/LOAD (KN)	15.2	20.2	25.2	30.2	40.2	20.2	35.2			
S/LOAD (KN)	10.0	12.0	15.0	18.0	24.0	10.0	22.0			

No. 5	c.s.a = 0.00221 m^2					No. 6	c.s.a = 0.00221 m^2			
N/LOAD (KN)	7.2	10.2	12.2	15.2	20.2	5.2	15.2	25.2	35.2	45.2
S/LOAD (KN)	4.5	7.0	9.0	12.5	14.5	2.5	12.0	15.5	24.0	29.0

APPENDIX D

SLOPE STABILITY ANALYSIS WITH PCSTABL5 VERSION

PCSTABL5 is the newest version of the STABL programs for the analysis of slope stability problems. It is written in FORTRAN, and it calculates the factor of safety against slope failure by a two-dimensional limiting equilibrium method. It employs the simplified Bishop method of slices for circular failure surfaces, the simplified Janbu method of slices for failure surfaces of a general shape or Spencer's method of slices for surfaces of circular or general shape.

PCSTABL5 features a unique technique for random generation of potential failure surfaces for the subsequent determination of the more critical failure surfaces and their corresponding factors of safety. Circular, irregular and sliding block surfaces may be generated and analyzed using either a random search technique or specific input of the coordinates of a given potential failure surface.

The user defines the slope geometry in rectangular coordinates, the rock/soil types with their corresponding shear strength parameters and specifies the method of analysis (circular, random or block) as input data. The program is capable of handling heterogeneous soil/rock

systems, anisotropic strength parameters, excess pore water pressures, static ground water, earth quake loading, surcharge and tieback loading.

Plotted outputs (see Figs.D1, D2 & D3) provide as visual aids to confirm the correctness of the problem input data and the location of the critical potential failure surfaces generated. The program calculates the factor of safety for each generated failure surface as specified by the user (usually more than 10 surfaces per initiation point are specified). For its output, however, only the TEN most critical potential failure surfaces with their factors of safety are listed starting with the most critical failure surface first.

oooooooooooooooooo

Fig. D-1 MOP 435 FLUOR -D27A- DESIGN CUT
SECTION 12E POS ANALYSIS (125 failure surfaces generated)

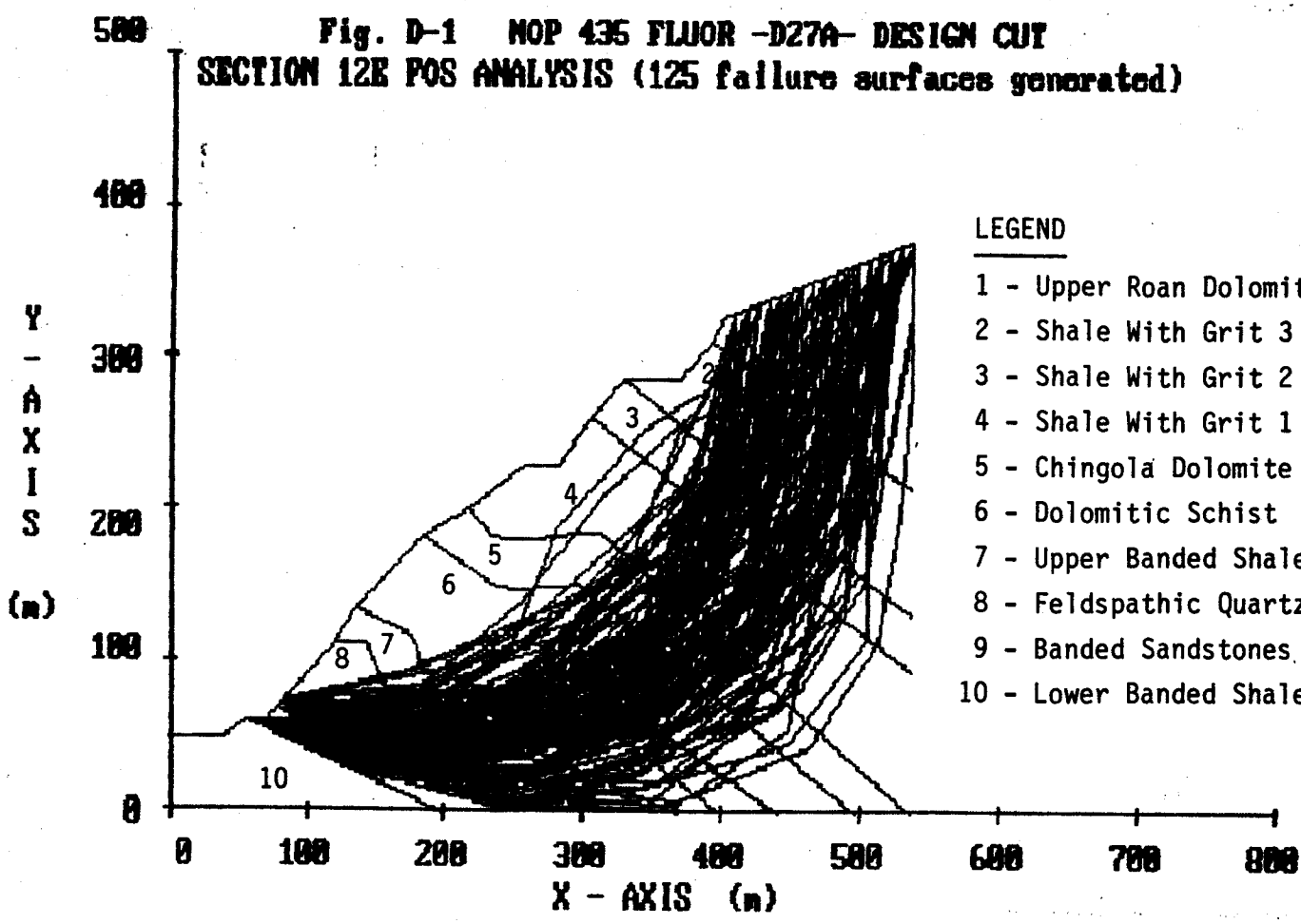

Fig. D-2 SECTION 12E FOS ANALYSIS:
F.O.S for TEN most CRITICAL surfaces (1.083 - 1.107)

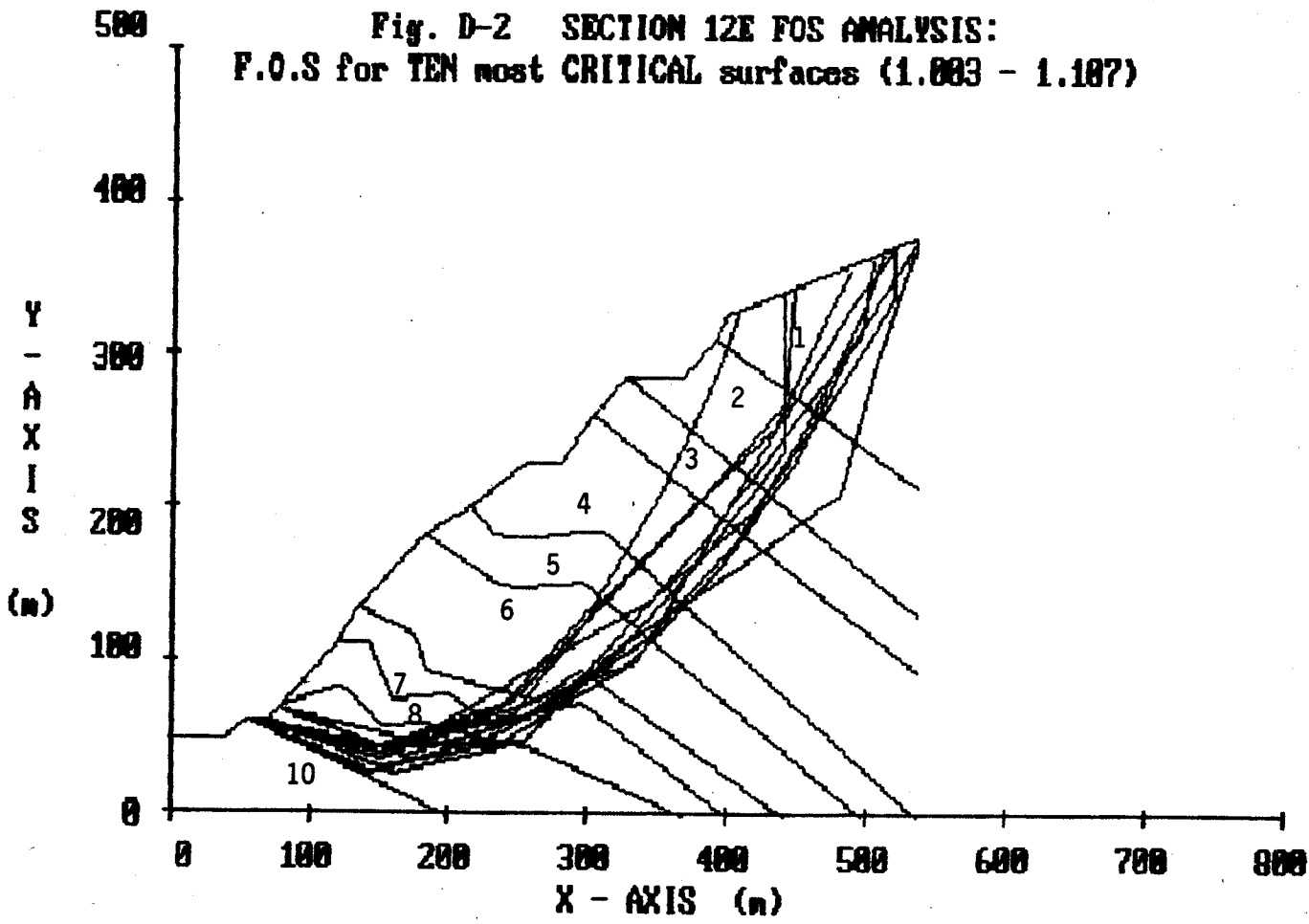

Fig. D-3 SECTION 12E FOS ANALYSIS:
POTENTIAL FAILURE SURFACE INITIATING in BSS (FOS = 1.883)